Loss of LOFSEP Transcription Factor Function Converts Spikelet to Leaf-Like Structures in Rice[1][OPEN]

Di Wu,[a] Wanqi Liang,[a] Wanwan Zhu,[a] Mingjiao Chen,[a] Cristina Ferrándiz,[b] Rachel A. Burton,[c] Ludovico Dreni,[a,b,2] and Dabing Zhang[a,c,2]

[a]Joint International Research Laboratory of Metabolic and Developmental Sciences, State Key Laboratory of Hybrid Rice, Shanghai Jiao Tong University-University of Adelaide Joint Centre for Agriculture and Health, School of Life Sciences and Biotechnology, Shanghai Jiao Tong University, Shanghai 200240, China
[b]Instituto de Biología Molecular y Celular de Plantas, Consejo Superior de Investigaciones Científicas-Universidad Politécnica de Valencia, Valencia 46022, Spain
[c]School of Agriculture, Food and Wine, University of Adelaide, Waite Campus, Urrbrae, SA 5064, Australia

ORCID IDs: 0000-0003-1101-1170 (D.W.); 0000-0002-9938-5793 (W.L.); 0000-0002-9079-5980 (M.C.); 0000-0002-2460-1068 (C.F.); 0000-0002-0638-4709 (R.A.B.); 0000-0002-2059-8420 (L.D.); 0000-0002-1764-2929 (D.Z.).

SEPALLATA (*SEP*)-like genes, which encode a subfamily of MADS-box transcription factors, are essential for specifying floral organ and meristem identity in angiosperms. Rice (*Oryza sativa*) has five *SEP*-like genes with partial redundancy and overlapping expression domains, yet their functions and evolutionary conservation are only partially known. Here, we describe the biological role of one of the *SEP* genes of rice, *OsMADS5*, in redundantly controlling spikelet morphogenesis. *OsMADS5* belongs to the conserved *LOFSEP* subgroup along with *OsMADS1* and *OsMADS34*. *OsMADS5* was expressed strongly across a broad range of reproductive stages and tissues. No obvious phenotype was observed in the *osmads5* single mutants when compared with the wild type, which was largely due to the functional redundancy among the three *LOFSEP* genes. Genetic and molecular analyses demonstrated that *OsMADS1*, *OsMADS5*, and *OsMADS34* together regulate floral meristem determinacy and specify the identities of spikelet organs by positively regulating the other MADS-box floral homeotic genes. Experiments conducted in yeast also suggested that OsMADS1, OsMADS5, and OsMADS34 form protein-protein interactions with other MADS-box floral homeotic members, which seems to be a typical, conserved feature of plant SEP proteins.

At present there are an estimated 352,000 species of angiosperms on Earth (The Plant List 2013), which have evolved a variety of inflorescences and flower morphologies (Theissen and Melzer, 2007). The monocot family of grasses (Poaceae) represents nearly one-fifth of all monocotyledons (Linder and Rudall, 2005) and includes many economically significant crops such as rice (*Oryza sativa*) and maize (*Zea mays*). Grasses have evolved a surprisingly diversified inflorescence structure and arrangement of spikelets and flowers, which not only differ from eudicot plants but also other monocots. The rice inflorescence meristem is determinate, because it arrests after producing a programmed number of primary and secondary branches, and panicle branching is an important agronomic trait for crop improvement. In all grasses, the basic inflorescence structural unit is the spikelet (Ciaffi et al., 2011; Zhang et al., 2013; Zhang and Yuan, 2014), which in rice contains only one floret and, arranged in a distichous pattern at its base, two highly reduced leaf-like rudimentary glumes and two depressed sterile lemmas (also called empty glumes) above the rudimentary glumes (Kellogg, 2001; Itoh et al., 2005; Yoshida and Nagato, 2011). In addition, rice florets have a bilateral symmetry with five types of floral organs with characteristic numbers, that is one bract-like lemma and one bract-like palea arranged in the adjacent outer whorls, the latter of which is hypothesized to be the first true floral whorl of grasses, two small fleshy organs called lodicules in the second whorl, six stamens in the third whorl, and one pistil in the fourth innermost whorl (Prasad et al., 2001; Prasad and Vijayraghavan, 2003; Zhang and Wilson, 2009; Ciaffi et al., 2011).

The classic ABC model of flower development in angiosperms was formulated more than 25 years ago (Coen and Meyerowitz, 1991). This model, which was based on the observation of mutants with defects in floral organ development, expounds how floral meristem (FM) determinacy and floral organ identity are genetically specified, and shows that the relatively distantly related eudicot flowering plants Arabidopsis (*Arabidopsis thaliana* L. Heynh.) and snapdragon (*Antirrhinum majus*) use conserved mechanisms in floral pattern regulation. In Arabidopsis, sepals form in floral whorl 1 because of expression of only the so-called class A genes (*APETALA1* [*AP1*] and *AP2*), whereas class A and class B (*AP3* and *PISTILLATA*) together direct petal development in whorl 2, B and C (*AGAMOUS* [*AG*]) together specify stamens in whorl 3, and class C genes expressed alone determine FM termination and carpel formation in the fourth and last whorl. More recently two gene classes, D and E, have been added to form an extended ABCDE model. The D-class gene (*SEEDSTICK* [*STK*]) controls the development of ovules (Pinyopich

et al., 2003), while four E-class genes *SEPALLATA1/2/3/4* (*SEP1/2/3/4*; formerly known as *AGL2/3/4/9*) specify the identities of all four whorls of floral organs and ovules and determine FM identity and determinacy (Pelaz et al., 2000; Pelaz et al., 2001; Favaro et al., 2003; Ditta et al., 2004). Except for *AP2*, all class A, B, C, D, and E genes encode MIKC-type MADS-box transcription factors.

These MADS-box proteins fall into different subfamilies whose functions are broadly conserved in angiosperms; thus, the ABCDE model can largely explain floral development in monocots such as grasses. Rice has four *AP1/FRUITFULL* (*FUL*)-like genes, *OsMADS14*, *OsMADS15*, *OsMADS18*, and *OsMADS20*, as putative class A genes (Kyozuka et al., 2000; Pelucchi et al., 2002; Fornara et al., 2004; Kater et al., 2006; Preston and Kellogg, 2006; Wu et al., 2017). The analysis of rice floral homeotic mutants for the *AP3*-like gene *OsMADS16/SUPERWOMAN1* and the *PI*-like genes *OsMADS2* and *OsMADS4* showed that the function of B-class genes is conserved from grasses to eudicots (Kang et al., 1998; Nagasawa et al., 2003; Prasad and Vijayraghavan, 2003; Yamaguchi et al., 2006; Yadav et al., 2007; Yoshida et al., 2007; Yao et al., 2008; Yun et al., 2013). In rice, there are two *AG* orthologous genes, *OsMADS3* and *OsMADS58*, and two *STK* orthologs, *OsMADS13* and *OsMADS21*, which function as class C and class D genes, respectively (Lopez-Dee et al., 1999; Kyozuka and Shimamoto, 2002; Yamaguchi et al., 2006; Dreni et al., 2007; Dreni et al., 2011; Hu et al., 2011). Grasses have diverse *SEP*-like genes divided into five conserved lineages, which are represented in rice by *OsMADS1*, *OsMADS5*, *OsMADS7* (allelic to *OsMADS45*), *OsMADS8* (allelic to *OsMADS24*), and *OsMADS34* (Greco et al., 1997; Kang et al., 1997; Malcomber and Kellogg, 2005; Zahn et al., 2005; Arora et al., 2007; Ciaffi et al., 2011). All the *SEP*-like genes of angiosperms form two major clades, the *LOFSEP* clade (also called *SEP1/2/4* clade or *AGL2/3/4* clade) comprising the rice genes *OsMADS1*, *OsMADS5*, and *OsMADS34*, and the *SEP3* clade (also called *AGL9* clade) including the two rice genes *OsMADS7(45)* and *OsMADS8 (24)* (Malcomber and Kellogg, 2005; Zahn et al., 2005; Arora et al., 2007). The rice *LOFSEP* gene *OsMADS1/LHS1* (*LEAFY HULL STERILE1*) was the first E-class gene to be partially characterized in grasses. *OsMADS1* controls differentiation of specific cell types in the lemma and palea and is an early-acting regulator of inner floral organs. The mutation of *OsMADS1* causes elongated leafy palea and lemmas, an open hull, two pairs of leafy palea- or lemma-like lodicules, the decrease of stamen number, the increase of carpel number, and an additional floret arising from the same rachilla (Jeon et al., 2000; Prasad et al., 2001, 2005; Agrawal et al., 2005; Hu et al., 2015). No obvious defect in either panicles or vegetative organs was observed in the loss-of-function mutation of the *LOFSEP* gene *OsMADS5*, except for the lodicules remaining more tightly attached to the lemma and palea upon spikelet dissection (Agrawal et al., 2005). The *LOFSEP* gene *OsMADS34* (*PANICLE PHYTOMER2* [*PAP2*]) is required for rice inflorescence and spikelet development (Gao et al., 2010; Kobayashi et al., 2010; Lin et al., 2014). The *osmads34-1* mutant displayed altered inflorescence morphology with increased primary branch number and decreased secondary branch number. Moreover, the *osmads34-1* mutant had fewer spikelets and altered spikelet morphology, with elongated sterile lemmas acquiring lemma/palea-like features (Gao et al., 2010). *OsMADS34/PAP2* is also involved in the transition from vegetative to reproductive growth through the specification of inflorescence meristem identity. Indeed, *OsMADS34* and three *AP1/FUL*-like genes, *OsMADS14*, *OsMADS15*, and *OsMADS18*, coordinately act in the meristem to specify inflorescence meristem, downstream of the florigen signal (Kobayashi et al., 2012). As for the members of the *SEP3* clade, knockdown of both *OsMADS7(45)* and *OsMADS8 (24)* showed severe phenotypes including late flowering, homeotic changes of lodicules, conversion of stamens and carpels into palea/lemma-like organs, and a loss of floral determinacy (Cui et al., 2010). Therefore, all of the above *SEP*-like floral homeotic genes in rice show both functional conservation (E function) and diversification. In addition, *AGL6* is an ancient subfamily of MADS-box genes, sister to the *SEP*s and comprising the rice genes *OsMADS6/MOSAIC FLORAL ORGANS1* and *OsMADS17* (Zahn et al., 2005; Ohmori et al., 2009). The characterization of rice *osmads6* mutant alleles indicated that the *AGL6*-like genes contribute to the E-function in floral development, like the *SEP* genes (Ohmori et al., 2009; Li et al., 2010, 2011; Zhang et al., 2010), and this has been observed in other angiosperms (Rijpkema et al., 2009; Thompson et al., 2009; Dreni and Zhang, 2016).

[1] This work was supported by the National Natural Science Foundation of China (NSFC) (31230051), the NSFC Research Fund for International Young Scientists (31550110198), the National Key Technologies Research and Development Program of China, Ministry of Science and Technology (grant no. 2016YFD 0100804; 2016YFE0101000), the H2020-MSCA-RISE-2015 project ExpoSEED (691109), the China Postdoctoral Science Foundation (2014M560328), the National Transgenic Major Program (grant no. 2016ZX08009003-003-007), the Innovative Research Team, Ministry of Education; the 111 Project (grant no. B14016), Australian Research Council (DP170103352), an Australia-China Science and Research Fund Joint Research Centre grant (ACSRF48187), and the National Key Technologies Research and Development Program of China, Ministry of Science and Technology (grant no. 2016YFD 0100804). L.D. is supported by a Marie Skłodowska-Curie Global Fellowship (H2020-MSCA-IF-2014_GF, proposal no. 661678 'RiceStyle').

[2] Address correspondence to zhangdb@sjtu.edu.cn and ludovico.dreni@gmail.com.

D.Z. and W.L. conceived the original research plans and provided the rice strains; D.W. performed most of the experiments; W.Z. performed CRISPR mutagenesis and maintained the lines; D.W. and M.C. generated the higher order mutant lines and grew the plants; D.W., D.Z., C.F., R.A.B., and L.D. designed the experiments and analyzed the data; D.W., L.D., C.F., R.A.B., and D.Z. wrote the article; all authors read and approved the final draft; L.D. and D.Z. supervised this work and completed the writing.

The authors responsible for distribution of materials integral to the findings presented in this article in accordance with the policy described in the Instructions for Authors (www.plantphysiol.org) are: Dabing Zhang (zhangdb@sjtu.edu.cn) and Ludovico Dreni (ludovico.dreni@gmail.com).

[OPEN] Articles can be viewed without a subscription.
www.plantphysiol.org/cgi/doi/10.1104/pp.17.00704

Although the class E floral homeotic genes in rice have already been studied to define their role in molecular mechanisms regulating flower development, the presence of the five *SEP* genes has been an obstacle in elucidating their global functions, as rice is a much less amenable model plant in which to construct higher order mutants, compared to Arabidopsis. Therefore, the function of *OsMADS5* and the genetic interactions among *SEP*-like genes are still largely unknown. In an effort to address this question, Cui et al. (2010) took an RNA interference (RNAi) knockdown approach targeting all rice *SEP* genes except *OsMADS34*, which led to the homeotic transformation of all floral organs except the lemma into leaf-like organs. However, the specific functions of the rice *LOFSEP* and *SEP3* clades are still not clear, although there is evidence of more functional divergence than in Arabidopsis, since the inhibition of just *OsMADS1* or *OsMADS34*, alone or of both these genes together, is sufficient to cause severe phenotypes (Jeon et al., 2000; Prasad et al., 2001, 2005; Agrawal et al., 2005; Cui et al., 2010; Gao et al., 2010; Kobayashi et al., 2010). To date, *OsMADS5* remains the less studied *SEP*-like gene in rice, where only one mutant allele has been generated, which suggested only a minor role for this gene in spikelet development (Agrawal et al., 2005).

In this study, we characterized the genetic interaction of the *LOFSEP* members *OsMADS1*, *OsMADS5*, and *OsMADS34* and explored their molecular mechanisms in controlling rice spikelet morphogenesis. To address this question, we used the stable mutant alleles *osmads1-z* (Gao et al., 2010; Hu et al., 2015) and *osmads34-1* (Gao et al., 2010) and we identified and characterized the new *osmads5-3* mutant allele. We constructed all possible double mutant combinations, namely *osmads1-z osmads34-1* (Gao et al., 2010), *osmads1-z osmads5-3*, and *osmads5-3 osmads34-1*, and the triple mutant *osmads1-z osmads5-3 osmads34-1*, to obtain a detailed comparison of their spikelet phenotypes. Altogether, our data reveal that *OsMADS5* is a key player in rice spikelet morphogenesis together with *OsMADS1* and *OsMADS34*. Moreover, genetic interaction analysis of the *LOFSEP* members *OsMADS1*, *OsMADS5*, and *OsMADS34* reveals their redundant role in regulating the identity of sterile lemma, lemma and palea, and also of all the inner floral organs, where their latter function is very likely to be dependent on the transcriptional activation of B-, C-, *AGL6*-, and *SEP3*-like genes. These new insights help to better understand the core genetic mechanisms underpinning floral development in rice and its conserved and diverged aspects across the evolution of angiosperms.

RESULTS

Identification of the *OsMADS5* T-DNA Insertion Mutant

We searched the rice T-DNA insertion library database (Rice Mutant Database, RMD) and identified one insertion line for the *OsMADS5* gene. The T-DNA was inserted in the seventh exon (Supplemental Fig. S1A). Because two *Tos17* insertion alleles were previously reported (Agrawal et al., 2005), we named this T-DNA mutant *osmads5-3*. Three pairs of primers for quantitative reverse transcription PCR (qRT-PCR) were used to quantify *OsMADS5* transcripts, revealing that the insertion caused a significant reduction of transcript when primer sets upstream of the T-DNA were used, but no transcript could be detected using the primer pair downstream of the T-DNA. It is therefore highly likely that most of the C terminus from the translated protein product was not present in *osmads5-3* plants (Supplemental Fig. S1, B–D). The *osmads5-3* line was subsequently backcrossed with its wild-type parent Zhonghua11 (*Oryza sativa* L. ssp. *japonica*) three times.

Expression Pattern of *OsMADS5*

Based on previous studies in rice, the developmental courses of inflorescence and spikelet development have been divided into nine and eight stages, respectively (Ikeda et al., 2004). qRT-PCR analysis revealed a broad expression pattern of *OsMADS5* in wild-type reproductive tissues. This included young inflorescences from 0.3 to 7 mm, which span the inflorescence and spikelet development stages from In3 to In5 and from Sp1 to Sp8, respectively, but also the mature sterile lemmas, lemmas, paleas, lodicules, anthers, and pistils at stage In8 to In9 when FM activity is terminated. No transcripts of *OsMADS5* were detected in vegetative tissues like roots or leaves (Fig. 1A). Subsequently, RNA in situ hybridization was performed to study the spatial distribution of *OsMADS5* mRNA, where faint signals indicated that *OsMADS5* mRNA accumulation was first detected at comparatively low levels in the rachis meristem and primary branch primordia during early inflorescence development (Fig. 1, D and E). Subsequently, the *OsMADS5* mRNA signal strengthened and was specific in the secondary branch meristem and spikelet meristem (SM) at stage In5 (Fig. 1F) and at the terminal and lateral SMs (Fig. 1G), persisting in the floret meristem during spikelet organogenesis. In spikelet and floral organs, *OsMADS5* was expressed at the tips of the rudimentary glumes and sterile lemmas as well as in the lemma primordia at stage Sp3 (Fig. 1H), then in lemma and palea primordia at stage Sp4, and finally in the primordia of lodicules, stamens, and carpels from stage Sp6 to Sp8 (Fig. 1, I–L).

OsMADS5 and *OsMADS34* Redundantly Regulate the Identity of Outer Spikelet Organs and Meristem Determinacy

A wild-type spikelet consists of two rudimentary glumes, two normal sterile lemmas, one lemma, one palea, two lodicules, six stamens, and one pistil (Fig. 2, A–D). Compared with the wild type, no obvious abnormal phenotype was detected in *osmads5-3* (Fig. 2, E–H), and the abnormal attachment of lodicules to lemma and palea previously reported for another *osmads5*

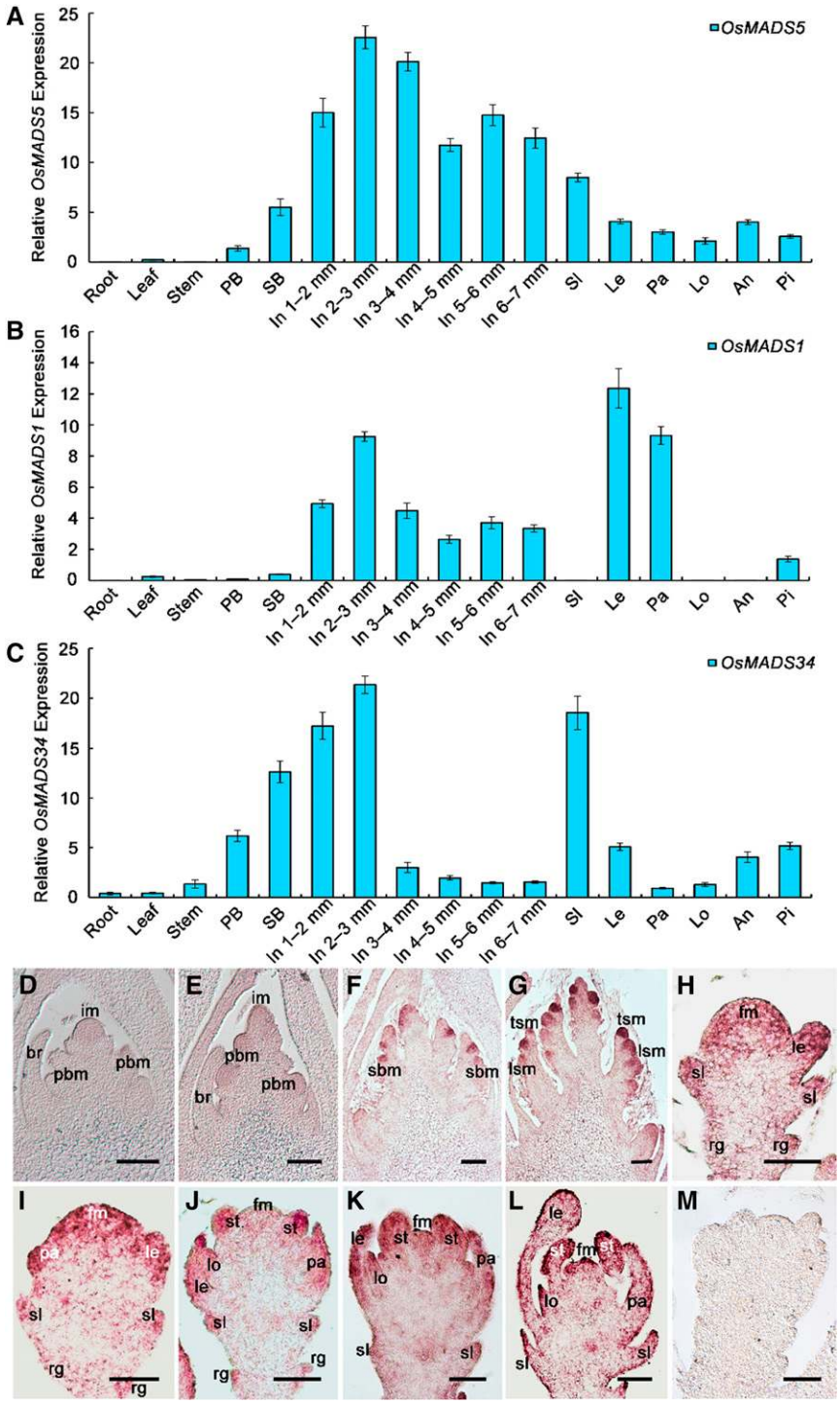

Figure 1. Expression pattern analysis of rice *LOFSEP* genes. A to C, qRT-PCR detection of *OsMADS5* (A), *OsMADS1* (B), and *OsMADS34* (C) transcripts. Total RNA was isolated from wild-type roots, leaves, stems, sterile lemmas, lemmas, paleas, lodicules, anthers, and pistils at stage In8 to In9 and also from 0.3- to 7-mm inflorescences. The inflorescence length around 0.3- to 0.6-mm covers the stages of In3 and In4 when the primary branches form and elongate, while inflorescence length 0.6 to 0.9 mm corresponds to stage In5 when the primary branch meristem produces secondary branches, but the SM has not yet formed. The results are presented as mean ± SD. Error bars indicate the SD for three biological replications. D to M, In situ hybridization analysis of *OsMADS5* expression in the wild type at stage In3 (D), In4 (E), In5 (F), early In6 (G), Sp3 (H), Sp4 (I), Sp6 (J), Sp7 (K), and Sp8 (L), and at stage Sp6 with sense control (M). an, anther; br, bract; fm, floral meristem; im, florescence meristem; In, inflorescence; le, lemma; lo, lodicule; lsm, lateral spikelet meristem; pa, palea; PB, primary branch; pbm, primary branch meristem; pi, pistil; rg, rudimentary glume; SB, secondary branch; sbm, secondary branch meristem; sl, sterile lemma; tsm, terminal spikelet meristem. Bars = 100 μm (D–G) and 50 μm (H–M).

mutant (Agrawal et al., 2005) was not observed. Since our T-DNA allele might not cause a complete loss of function of *OsMADS5*, we recently analyzed mutant lines created by the CRISPR/Cas9 system, which contained the mutations in the first or the second exon of *OsMADS5*, respectively (Supplemental Fig. S1A). Again, these lines did not show any visible floral phenotype compared with the wild type (Supplemental Fig. S5; Supplemental Tables S6 and S7), suggesting that the putative function of *OsMADS5* might be completely hidden by genetic redundancy. Indeed, dramatically stronger phenotypes were scored for the double and triple mutants described below, carrying the homozygous T-DNA insertion in the *OsMADS5* gene.

To investigate the genetic interaction between *OsMADS5* and *OsMADS34*, we crossed *osmads5-3* with

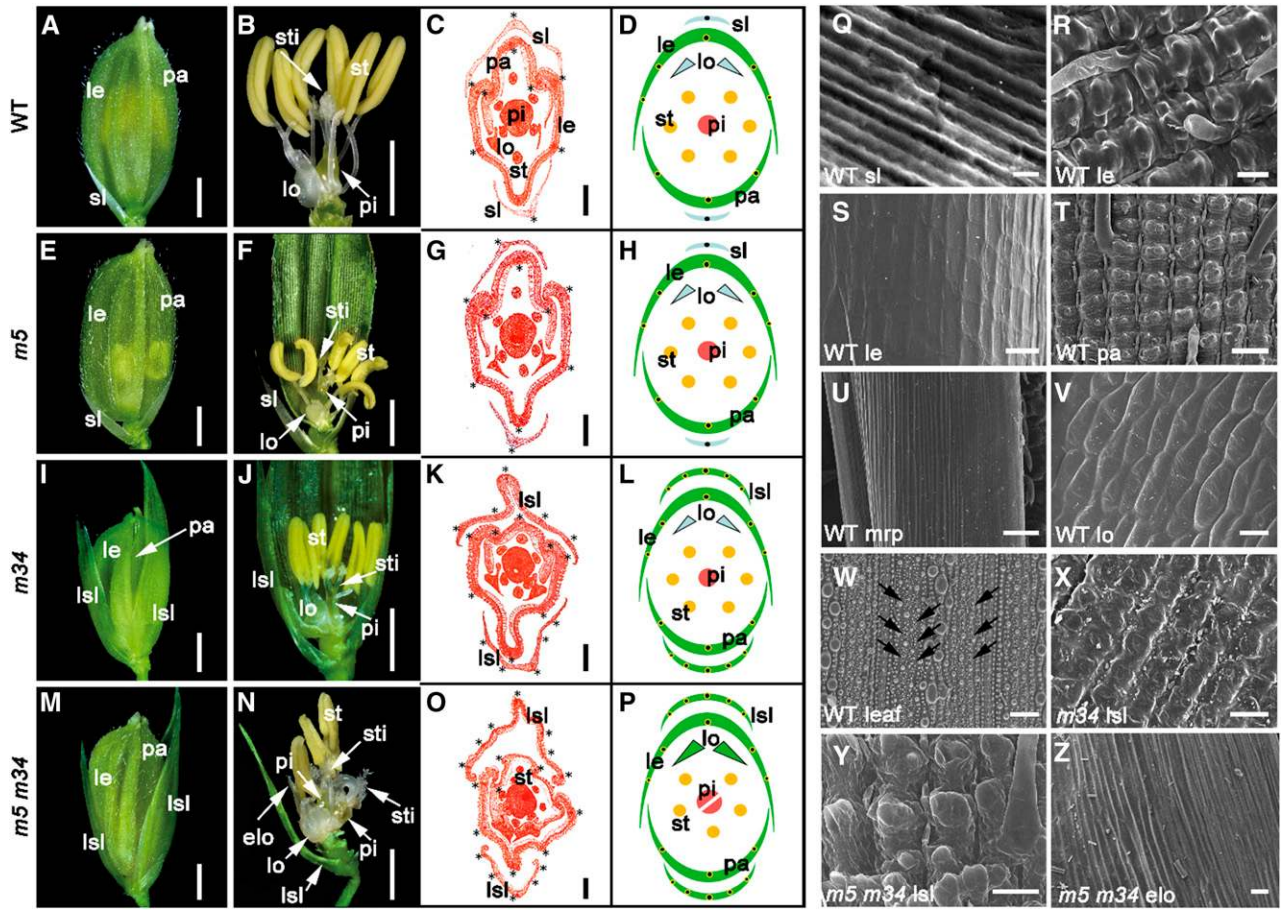

Figure 2. Phenotypes of wild type, *osmads5-3*, *osmads34-1*, and *osmads5-3 osmads34-1* mutants. A, E, I, and M, Spikelets of wild type (A), *osmads5-3* (E), *osmads34-1* (I), and *osmads5-3 osmads34-1* (M) at stage In9. B, F, J, and N, Lemma and palea were removed in wild type (B) and *osmads5-3 osmads34-1* (N) and half the lemma and palea were removed in *osmads5-3* (F) and *osmads34-1* (J) to show the inner floral organs of A, E, I, and M, respectively. C, G, K, and O, Transverse section of wild type (C), *osmads5-3* (G), *osmads34-1* (K), and *osmads5-3 osmads34-1* (O) at stage In9 showing the identity change of sterile lemma and defects of inner floral organs in the mutants. Black stars mark the number of vascular bundles. D, H, L, and P, Diagrammatic representation of wild-type (D), *osmads5-3* (H), *osmads34-1* (L), and *osmads5-3 osmads34-1* (P) spikelets. Q to Z, SEM analysis of the abaxial epidermis of wild-type sterile lemma (Q), lemma (R), palea (T), marginal region of palea (mrp) (U), lodicule (V), leaf blade (W), adaxial surface of wild type lemma (S), abaxial epidermis of lemma/palea-like sterile lemma of *osmads34-1* (X), and *osmads5-3 osmads34-1* (Y), and the abnormal elongated lodicule of *osmads5-3 osmads34-1* with an mrp-like structure (Z). Black arrowheads indicate the stomata. elo, elongated lodicule; le, lemma; lo, lodicule; lsl, lemma/palea-like sterile lemma; *m5*, *osmads5-3*; *m34*, *osmads34-1*; pa, palea; pi, pistil; sl, sterile lemma; st, stamen; sti, stigma. Bars = 2 mm (A, B, E, F, I, J, M, and N), 200 μm (C, G, K, and O), 50 μm (R, S, T, U, W, and Y), and 10 μm (Q, V, X, Z).

the previously identified mutant *osmads34-1* (Gao et al., 2010) to generate the double mutant. Consistent with previous reports, the defects observed in *osmads34-1* were limited to the conversion of sterile lemmas into elongated lemma/palea-like structures (Fig. 2, I–L), also consistent with the phenotype of CRISPR lines targeting the second exon of *OsMADS34* (Supplemental Figs. S1E and S5; Supplemental Tables S6 and S7). The *osmads5-3 osmads34-1* double mutant displayed a similar phenotype to the *osmads34-1* single mutant, except the lemma/palea-like structures were even longer and, in addition, new abnormalities appeared in the lemma, palea, and inner whorls of floral organs, such as elongated lodicules and a change in the number of stamens and pistils (Fig. 2, M–P).

These differences were quantified, showing that *osmads5-3 osmads34-1* displayed significantly longer lemma/palea-like sterile lemmas (12.01 $\pm$ 0.64 mm, n = 100) compared to *osmads34-1* (9.01 $\pm$ 0.32 mm, n = 100), to *osmads5-3* (3.12 $\pm$ 0.09 mm, n = 100), and to the wild type (3.12 $\pm$ 0.08 mm, n = 100; Supplemental Figs. S2 and S4B). There was also a modest increase in vascular bundle numbers per sterile lemma (5.27 $\pm$ 0.45, n = 30) compared with *osmads34-1* (5.00 $\pm$ 0.00, n = 30), *osmads5-3* (1.00 $\pm$ 0.00, n = 30), and the wild type (1.00 $\pm$ 0.00, n = 30), respectively (Supplemental Table S5).

The lemma/palea length of *osmads5-3 osmads34-1* was 8.87 ± 0.24 mm (n = 100), which was significantly longer than the wild type, and each of the *osmads5-3* and *osmads34-1* single mutant (Supplemental Figs. S2 and S4A). About 59.56% (n = 273) of *osmads5-3 osmads34-1* spikelets exhibited abnormal elongated lodicules in the second whorl (Supplemental Table S1). The stamen number in *osmads5-3 osmads34-1* fluctuated, but the average number of stamens per spikelet was 5.89 ± 0.87 (n = 273; Supplemental Figure S4, C–F; Supplemental Table S1). In addition, the average number of pistils and stigmas in *osmads5-3 osmads34-1* was 1.05 ± 0.26 (n = 273) and 2.55 ± 0.83 (n = 273) per spikelet, respectively, displaying a statistically significant increase compared with the wild type and with the two single mutants *osmads5-3* and *osmads34-1* (Supplemental Fig. S4, C–F; Supplemental Table S1).

Scanning electron microscopy (SEM) analysis was performed to examine abnormalities in *osmads5-3 osmads34-1* in detail. For *osmads5-3 osmads34-1*, the variation in the number of stamen primordia was obvious at Sp6 and the sterile lemmas were larger at Sp8, compared to the wild type and the two single mutants *osmads5-3* and *osmads34-1* (Supplemental Fig. S3, A–D). Unlike the sterile lemmas of the wild type with a smooth epidermal surface (Fig. 2Q), the abaxial (outer) epidermal surface of *osmads5-3 osmads34-1* and *osmads34-1* displayed a pattern with regularly arrayed bulges (Fig. 2, X and Y), which showed obvious similarities with the abaxial epidermal surface of wild-type lemma/palea (Fig. 2, R and T), suggesting a homeotic transformation of each sterile lemma into a lemma/palea-like structure. In the second whorl of *osmads5-3 osmads34-1* spikelets, the abaxial epidermal surface in most of the elongated lodicules exhibited a normal cellular morphology compared with the wild type, while occasionally displaying conversion to a structure resembling the marginal region of the palea (mrp) (Fig. 2, U, V and Z).

Taken together, these phenotypes reveal redundant regulatory roles of *OsMADS5* and *OsMADS34* not only in the outer bracts, that is the sterile lemmas, lemma, and palea, but also in the three innermost whorls of floral organs. Thus, *OsMADS5* and *OsMADS34* redundantly specify the identity of the sterile lemmas, lemma/palea, and lodicules as well as control the number of stamen and carpel primordia through the maintenance of meristem determinacy.

Osmads5-3 Partially Rescues the Defects of *osmads1-z* in the Second Whorl

To investigate the genetic interaction between *OsMADS5* and *OsMADS1*, we generated a double

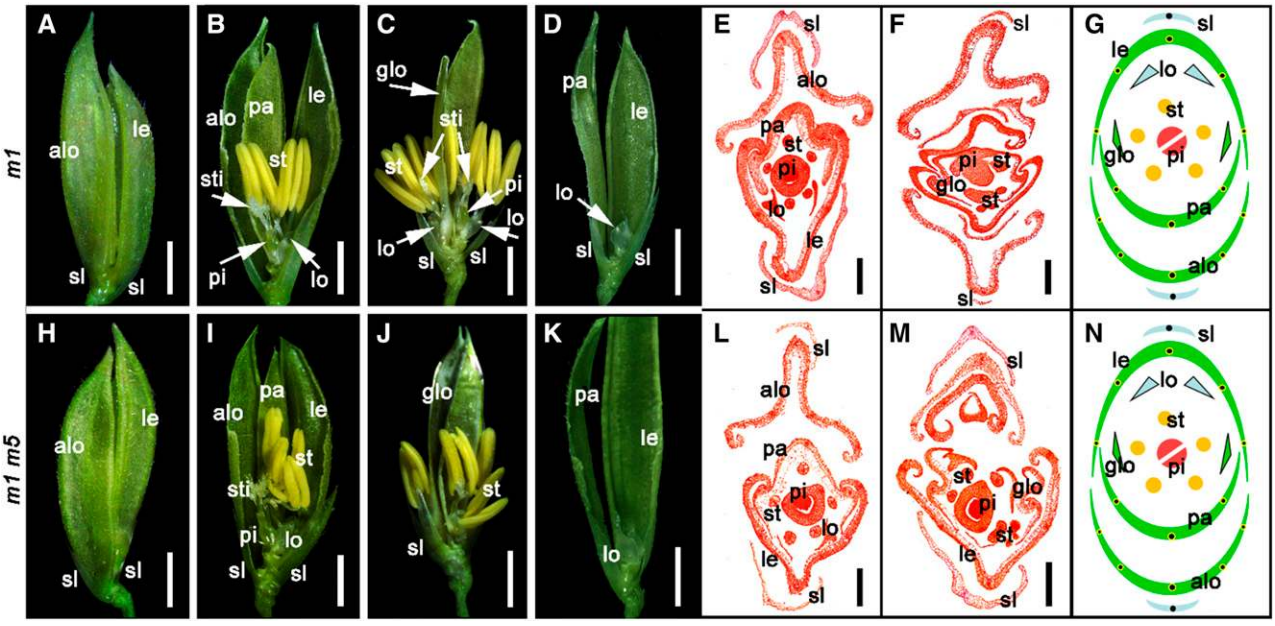

Figure 3. Phenotypes of *osmads1-z* and *osmads1-z osmads5-3* mutants. A and H, Spikelets of *osmads1-z* (A) and *osmads1-z osmads5-3* (H) at stage In9. B to D and I to K, The whole lemma and palea were removed in *osmads1-z* (C) and *osmads1-z osmads5-3* (J) spikelets with type II phenotype; half the lemma, palea, and additional lemma/palea-like organs were removed in *osmads1-z* (B) and *osmads1-z osmads5-3* (I) spikelets with type I phenotype; and half the lemma and palea were removed in osmads1-z (D) and *osmads1-z osmads5-3* (K) spikelets with type III phenotype to show the inner floral organs at stage In9. E, F, L, and M, Transverse section of *osmads1-z* with type I phenotype (E) and type II phenotype (F) and *osmads1-z osmads5-3* with type I phenotype (L) and type II phenotype (M) at stage In9 showing the defects in spikelets. G and N, Diagrammatic representations of *osmads1-z* (G) and *osmads1-z osmads5-3* (N) spikelets. alo, additional lemma/palea-like organ; glo, extra glume-like second whorl organ; le, lemma; lo, lodicule; *m1*, *osmads1-z*; *m5*, *osmads5-3*; pa, palea; pi, pistil; sl, sterile lemma; st, stamen; sti, stigma. Bars = 2 mm (A–D and H–K) and 200 μm (E, F, M, and N).

mutant by crossing *osmads5-3* with the previously identified mutant *osmads1-z* (Gao et al., 2010). Based on the previous analysis of *OsMADS1* mutants (Jeon et al., 2000; Agrawal et al., 2005; Prasad et al., 2005; Chen et al., 2006; Gao et al., 2010; Khanday et al., 2013) and on their inner organ defects, we grouped the various phenotypes of *osmads1-z* into five types in our study (Supplemental Table S2): Type I (77.54%, $n = 187$) was classified as a weak phenotype with an additional lemma/palea-like organ, normal lodicules on the lemma side and/or an extra pair of glume/mrp-like organs in the second whorl, a decreasing number of stamens, and an increasing number of carpels and stigmas (Fig. 3, A, B and E; Supplemental Fig. S3E). Type II (1.60%, $n = 187$) was represented by twin florets closely packed together (Fig. 3, C and F); type III (6.95%, $n = 187$) had normal lodicules inside the lemma and palea but lacked any stamens and pistil (Fig. 3D); type IV (13.37%, $n = 187$) displayed a complete loss of the inner three whorls of floral organs, and finally type V (0.53%, $n = 187$) had an additional new spikelet borne on an elongated pedicel (Supplemental Fig. S3E2). The phenotypes of the *osmads1-z osmads5-3* double mutant were very similar to the single *osmads1-z*, so they were also classified into five types (Fig. 3, H–M; Supplemental Fig. S3F). About 74.33% ($n = 187$) and 9.63% ($n = 187$) of the spikelets of *osmads1-z osmads5-3* exhibited the type I and type III phenotypes, respectively (Supplemental Table S2). In the second whorl, the total number of organs per spikelet (1.94 ± 0.65, $n = 143$) in *osmads1-z osmads5-3* did not change significantly compared with *osmads1-z* (1.99 ± 0.70, $n = 149$), whereas the ratio of normal lodicules to extra glume/mrp-like organs appeared remarkably altered (Supplemental Table S3). In the second whorl of *osmads1-z*, approximately 34.22% of the spikelets examined displayed normal lodicules, and the average number per spikelet of these lodicules was reduced to 0.81 ± 0.96 ($n = 149$), whereas 65.78% of the spikelets showed the abnormal extra glume-like organs at an average number of 1.19 ± 0.92 ($n = 149$). While in *osmads1-z osmads5-3*, a reduced percentage (only 37.76%) of the spikelets presented the extra glume-like organs with the significantly decreased average number of 0.60 ± 1.10 ($n = 143$), and the remaining 62.24% of the spikelets showed normal lodicules with the significantly increased average number of 1.27 ± 0.91 ($n = 143$; Supplemental Table S3). These results suggested that simultaneous mutation of both *OsMADS5* and *OsMADS1* can partially rescue the second whorl defects of *osmads1-z*, yet no significant differences were noticed in the other spikelet organs between *osmads1-z osmads5-3* and *osmads1-z*.

OsMADS5, *OsMADS1*, and *OsMADS34* Together Determine the Spikelet Identity

To investigate the reproductive roles of the three *LOFSEP*-like members *OsMADS5*, *OsMADS1*, and *OsMADS34*, we further generated the *osmads1-z osmads5-3 osmads34-1* triple mutant and reanalyzed the *osmads1-z osmads34-1* double mutant that was identified previously (Gao et al., 2010) as a control, because among the double mutant combinations it was the most similar to the triple mutant. *OsMADS1* is not expressed in the sterile lemmas of wild type, but its expression has been reported in the lemma/palea-like sterile lemmas of *osmads34-z* mutants (Ren et al., 2016). Consistently, the *osmads1-z osmads34-1* spikelet displayed abnormally elongated and leafy sterile lemmas and lemma/palea. It also showed both extra leaf/glume/mrp-like organs and normal lodicules in the second whorl, plus a decreased number of stamens and increased number of pistils compared with the wild type and each single mutant of *osmads1-z* and *osmads34-1* (Fig. 4, A and C). The *osmads1-z osmads5-3 osmads34-1* triple mutant displayed more severe defects of the spikelet organs, including the significantly elongated leafy sterile lemmas (15.61 ± 1.41 mm, $n = 100$) and lemma/palea (38.08 ± 5.46 mm, $n = 100$) compared to those of *osmads1-z osmads34-1* at an average length of 9.08 ± 0.31 mm ($n = 100$) and 17.90 ± 2.17 mm ($n = 100$), respectively (Fig. 4B; Supplemental Figs. S2 and S4, A and B). Moreover, for *osmads1-z osmads5-3 osmads34-1*, the average number of vascular bundles per sterile lemma (6.75 ± 0.85, $n = 20$) and per lemma/palea (13.06 ± 1.26, $n = 20$) were also notably increased compared to *osmads1-z osmads34-1* with an average number of 6.00 ± 0.73 ($n = 20$) and 9.75 ± 1.64 ($n = 20$), respectively (Fig. 4, I–N; Supplemental Table S5). These differences suggest that a more severe homeotic transformation of the sterile lemma and lemma/palea into leaves occurred in the triple mutant. A further reduction of organs occurred in the inner three whorls of *osmads1-z osmads5-3 osmads34-1*, including a reduced number of elongated glume-like organs arranged in the second whorl, and the sharply reduced number of stamens, pistils, and stigmas (1.51 ± 0.80 1.28 ± 0.93 and 2.50 ± 1.67, respectively, $n = 103$) in comparison with *osmads1-z osmads34-1* (Fig. 4, C–F; Supplemental Fig. S4, C–F; Supplemental Table S4). Also visible was the growth of undifferentiated tissues or a cluster of additional FMs defective in determinacy (Fig. 4, G, M, and N) instead of the determinate FMs of *osmads1-z osmads34-1*. In addition, the total number of leaf-like lemmas/paleas per spikelet was significantly increased in *osmads1-z osmads5-3 osmads34-1* (3.54 ± 0.50, $n = 103$) compared with *osmads1-z osmads34-1* (2.00 ± 0.00, $n = 102$) and the wild type (2.00 ± 0.00, $n = 200$), resulting in an increased total number of outer spikelet organs including the sterile lemmas and the lemma/paleas (5.86 ± 0.67, $n = 103$, occasionally up to 11 in the most severely affected spikelets; Fig. 4H; Supplemental Table S4). This suggested the homeotic transformation of floral organs of the inner three whorls into outer whorl/leaf-like organs in *osmads1-z osmads5-3 osmads34-1*, or, alternatively, a delay in the switch of SM into FM leading to a consequent reiteration of outer whorls.

SEM analysis was used to gain a better understanding of the identity of the aberrant spikelet organs

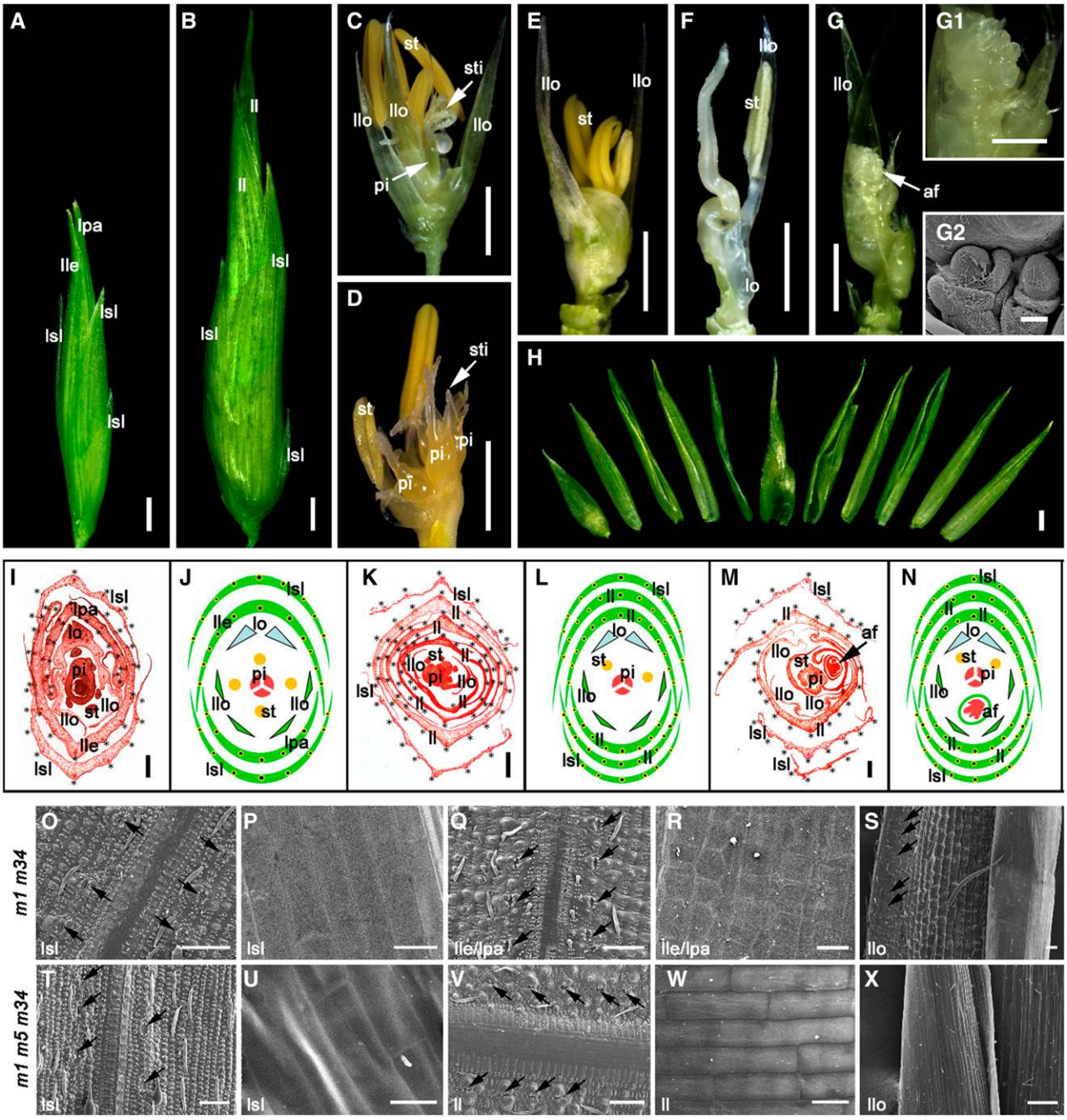

Figure 4. Phenotypes of *osmads1-z osmads34-1* and *osmads1-z osmads5-3 osmads34-1* mutants. A and B, Spikelets of *osmads1-z osmads34-1* (A) and *osmads1-z osmads5-3 osmads34-1* (B) at stage In9. C to G, Elongated leaf-like sterile lemma, lemma and palea were removed in *osmads1-z osmads34-1* (C) and *osmads1-z osmads5-3 osmads34-1* (D–G) to show the inner floral organs at stage In9. G1, A close-up view of the additional floral meristems marked by white arrowheads in G. G2, SEM analysis of the additional floral meristems marked by white arrowheads in G. H, All the leaf-like sterile lemmas, lemmas and paleas which were dissected from the same spikelet shown in G to show the increased number of outer spikelet organs in *osmads1-z osmads5-3 osmads34-1*. I, K, and M, Transverse section of *osmads1-z osmads34-1* (I) and *osmads1-z osmads5-3 osmads34-1* (K and M) at stage In9. Black stars mark the number of vascular bundles. J, L, and N, Diagrammatic representations of *osmads1-z osmads34-1* (J) and *osmads1-z osmads5-3 osmads34-1* (L and M) spikelets. O to S, SEM analysis of the abaxial epidermis of *osmads1-z osmads34-1* leaf-like sterile lemma (O), leaf-like lemma/palea (Q), and a mixed epidermal pattern of extra second whorl organs consisting of leaf-like (left side), lemma/palea-like (middle), and a marginal region of the palea-like (mrp-like) structures (right side) (S), and the inner/adaxial surface of leaf-like sterile lemma (P) and lemma/palea (R). T to X, SEM analysis of the abaxial epidermis of *osmads1-z osmads5-3 osmads34-1* leaf-like sterile lemma (T), leaf-like lemma/palea (V), mrp-like extra lodicules (X), and the adaxial surface of leaf-like sterile lemma (U) and lemma/palea (W). Black arrowheads indicate the

observed in the mutants. During spikelet development, *osmads1-z osmads5-3 osmads34-1* sterile lemmas and lemma/palea were already abnormally enlarged at Sp6 and Sp8, as seen in *osmads1-z osmads34-1* (Supplemental Fig. S3, G2–G4, and H3–H4), but more defects were detected inside the triple mutant spikelet, such as double FMs (Supplemental Fig. S3H2). Because sterile lemmas and lemma/palea had a leafy appearance in the mutants, we compared them with mature leaves. In wild-type leaf blades, the abaxial (lower) epidermal surface showed small bulges and several ordered lines of stomata along both sides of each vein (Fig. 2W). For *osmads1-z osmads5-3 osmads34* and *osmads1-z osmads34-1*, the corresponding abaxial (outer) epidermal surface of the elongated sterile lemmas and lemma/palea exhibited similar patterns to wild-type leaf blades, except that only one line of stomata was found along both sides of each vein (Fig. 4, O, Q, T, and V), while the adaxial (inner) surface displayed smooth rectangular cells reminiscent of the lemma and palea adaxial surface rather than the adaxial (upper) leaf blade surface (Figs. 2S and 4, P, R, U, and W). These results indicated a partial homeotic transformation of the sterile lemma and lemma/palea to leaf-like structures in the double and triple mutant, especially on the adaxial side. The outer surface of the elongated glume-like second whorl organs was also examined, and a mixed epidermal pattern consisting of leaf-like, lemma/palea-like, and mrp-like structures was observed in *osmads1-z osmads34-1* (Fig. 4S). However, only mrp-like cells were observed in the corresponding ectopic organs of the triple mutant (Fig. 4X), revealing that the mutation of *OsMADS5* reduced the range of second whorl defects in *osmads1-z osmads34-1* double mutants. The results above indicated that the three *LOFSEP*-like members *OsMADS5*, *OsMADS1*, and *OsMADS34* together regulate the identity of sterile lemma, lemma, palea, and lodicule and the determinacy of FM and determine the correct initiation of stamen and pistil.

LOFSEP Genes Positively Regulate the Expression of Floral Homeotic Genes

To further study the regulatory function of rice *LOFSEP* members, qRT-PCR was performed to measure transcript levels of most of the other MADS-box genes known to be involved in flower development. Young inflorescences from 2 mm to 7 mm long were examined in the *lofsep* mutants and the wild type, covering five developmental time points across spikelet development, from Sp4 to Sp8.

The transcripts of two *AP1/FUL*-like genes *OsMADS14* and *OsMADS15* were marginally increased in *lofsep* mutants, in particular in the triple mutant, compared with their parental varieties Zhonghua11 and 9522 (Fig. 5, A and B).

The expression levels of other floral homeotic genes, that is the two *SEP3*-like genes *OsMADS7(45)* and *OsMADS8(24)*, the *PI*-like gene *OsMADS4*, the *AP3*-like gene *OsMADS16*, and the two *AG* lineage genes *OsMADS3* and *OsMADS58* were significantly decreased in *osmads1-z*, especially in the early stages, but did not change significantly in the *osmads5-3* and *osmads34-1* single mutants. Similarly, compared to *osmads1-z*, the expression level of these homeotic genes did not show obvious changes in *osmads1-z osmads5-3* or *osmads1-z osmads34-1*, except for *OsMADS58* at extremely low levels in the latter. But in the *osmads5-3 osmads34-1* double mutant, all genes tested were strongly suppressed across all developmental stages examined (Fig. 5, C–F, I and J). The *AGL6*-like genes *OsMADS6* and *OsMADS17* were down-regulated significantly only at the earliest developmental stages in *osmads1-z* and all the double mutants, except for *OsMADS17*, which was strongly down-regulated in *osmads5-3 osmads34-1* from stage Sp4 to Sp8 (Fig. 5, G and H). In the *osmads1-z osmads5-3 osmads34-1* triple mutant, *SEP3*-, *PI*-, *AP3*-, *AG*-, and the *AGL6*-like genes were strongly suppressed, except for *OsMADS3* in 4 to 5-mm and 5 to 7-mm panicles (spikelet stages Sp7 and Sp8; Fig. 5, C–J).

Subsequently, the expression of the *LOFSEP* genes themselves was examined in their mutant backgrounds. According to our previous work, no notable change in the amount of *OsMADS34* transcript was detected in the *osmads34-1* frame-shift mutant, which is caused by a change in the 3′ acceptor splice site in the fifth intron of the gene (Gao et al., 2010). In contrast, *OsMADS34* was moderately up-regulated in *osmads1-z*, consistently with previous data (Khanday et al., 2013), and also in *osmads1-z osmads5-3*, *osmads1-z osmads34-1*, and *osmads1-z osmads5-3 osmads34-1* (Fig. 6B). The *OsMADS1* transcript was not detectable in any mutant background that included *osmads1-z*, confirming that *osmads1-z* is a full knock-out mutant. Interestingly, *OsMADS1* was down-regulated in the *osmads5-3 osmads34-1* double mutant, suggesting that *OsMADS5* and *OsMADS34* may act redundantly as positive regulators of *OsMADS1* (Fig. 6A). Two pairs of primers were used to detect the *OsMADS5* transcripts in the *lofsep* mutants, either upstream (Fig. 6C) or downstream (Fig. 6D) of the T-DNA insertion site in *osmads5-3*, respectively. The *OsMADS5* transcript was decreased when amplified using the upstream primer set (Fig. 6C) and was depleted using the downstream primer set (Fig. 6D) in all of the mutant combinations involving *osmads5-3* but was not altered in *osmads1-z* and *osmads34-1* single or double mutants.

Figure 4. (*Continued.*)
stomata. af, additional floral meristems; ll, leaf-like lemma/palea; lle, leaf-like lemma; llo, leaf/glume/mrp-like second whorl organ; lpa, leaf-like palea; lsl, leaf-like sterile lemma; *m1*, *osmads1-z*; *m5*, *osmads5-3*; *m34*, *osmads34-1*; pi, pistil; st, stamen; sti, stigma. Bars = 2 mm (A–H), 1 mm (G1), 200 μm (I, K, and M), 50 μm (G2, O, Q, S, T, V, and X), and 20 μm (P, R, U, and W).

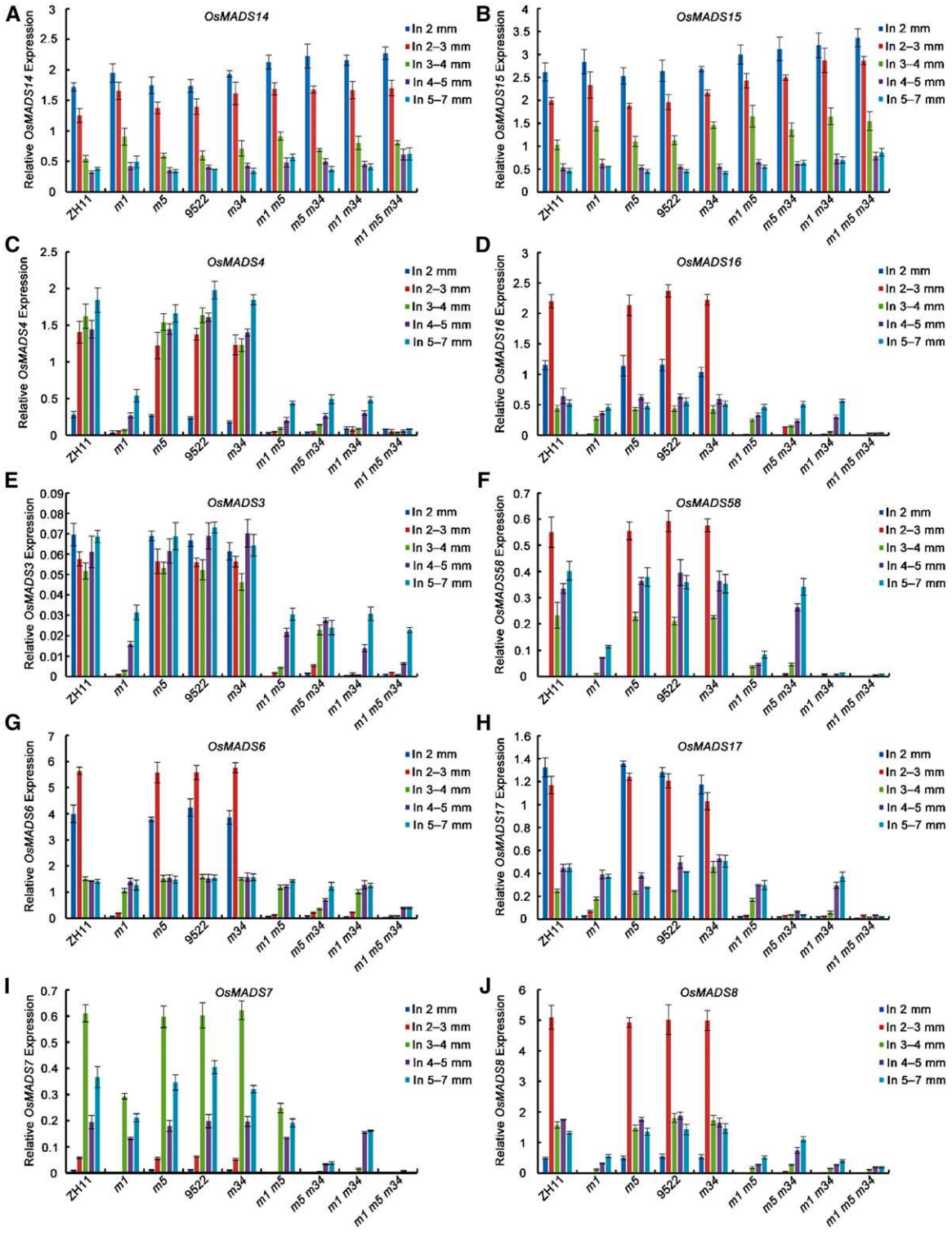

Figure 5. Expression analysis of some floral homeotic genes in the young panicles of *lofsep* mutants and the wild-type backgrounds. A to J, Expression levels of class A (*OsMADS14* and *OsMADS15*) (A and B), class B (*OsMADS4* and *OsMADS16*) (C and D), class C (*OsMADS3* and *OsMADS58*) (E and F), *AGL6*-like (*OsMADS6* and *OsMADS17*) (G and H), and *SEP3*-like (*OsMADS7* and *OsMADS8*) (I and J) genes were detected by qRT-PCR. Total RNA was isolated from 2- to 7-mm young inflorescences of the mutants of *osmads1-z*, *osmads5-3*, *osmads34-1*, *osmads1-z osmads5-3*, *osmads5-3 osmads34-1*, *osmads1-z osmads34-1*, and *osmads1-z osmads5-3 osmads34-1* and also the wild-type parents Zhonghua11 and 9522. The results are presented as mean ± SD.

These results suggested that rice *LOFSEP* members act, mostly redundantly, as upstream activators of B- and C-class genes as well as of *AGL6*-like and *SEP3*-like genes. *LOFSEP* genes may regulate the expression of each other, in particular *OsMADS5* and *OsMADS34* seem to promote *OsMADS1*, which in turn could be involved in the fine tuning of *OsMADS34* expression.

Physical Interactions of OsMADS5 and OsMADS34 with Other Floral Homeotic Proteins

In Arabidopsis, the identity of the different floral organs, sepals, petals, stamens, and carpels is determined by four combinations of floral homeotic MADS-box proteins, as described by the "quartet model" of floral organ specification (Theissen and Saedler, 2001). Therefore, we performed yeast two-hybrid assay to investigate whether OsMADS5 and OsMADS34 can interact with other MADS-box proteins. We found that OsMADS34 is able to form homodimers, in contrast to OsMADS5, while all the three LOFSEP-like members could interact with each other to form heterodimers. Both OsMADS5 and OsMADS34 could form heterodimers with other A-, B-, C-, D-, and E-class as well as AGL6-like proteins including OsMADS7(45), OsMADS8(24), OsMADS6, OsMADS14, OsMADS15, OsMADS2, OsMADS4, OsMADS16, OsMADS3, OsMADS58, and OsMADS13, respectively, albeit the interaction with OsMADS2 and OsMADS16 appeared weak (Fig. 7). These results suggested that the two LOFSEP proteins OsMADS5 and OsMADS34 have the ability to form higher order complexes together with class A, B, C, D, E, or AGL6-like proteins to control multifarious transcriptional programs required for flower development.

DISCUSSION

LOFSEP Genes Are Key Regulators of Rice Spikelet Organogenesis

In recent years, the function of *SEP*-like genes has gradually been characterized in rice. *OsMADS7(45)* and *OsMADS8(24)* are functionally redundant genes whose simultaneous silencing affects the development of only lodicules, stamens, and carpels in the innermost three whorls, consistent with their expression pattern (Cui et al., 2010).

OsMADS34 has been shown to be a key regulator of rice inflorescence architecture and of sterile lemma identity (Gao et al., 2010; Kobayashi et al., 2010, 2012). In our present study, the mutation of both *OsMADS5* and *OsMADS34* caused not only an increase in outer whorl defects greater than the mutation of *OsMADS34* alone, but also affected the inner whorls. Thus, there was an increased number of organs in the second whorl that acquired a palea-like identity rather than resembling lodicules, a variable number of stamens, and an increased number of carpels in the innermost two whorls. The number of stigmas also increased, due to the extra carpels and also because most carpels had more than two stigmas. This mimics the defects in the three inner whorls caused by the double knockdown of *OsMADS7(45)* and *OsMADS8(24)* (Cui et al., 2010) and also resembles the mild phenotype of *osmads1-z*. These phenotypes correlate strongly with the sharp decrease and delay of the onset of expression of *OsMADS7(45)* and *OsMADS8(24)*, along with B function, C function, and *AGL6*-like genes, during spikelet formation in the *osmads1-z* and *osmads5-3 osmads34-1* plants (Fig. 5, C–J). The phenotypic defects of the *osmads5-3 osmads34-1* double mutant reveal the functional redundancy between the two genes, as suggested by their sequence similarity and their highly overlapping expression patterns during spikelet organogenesis.

Our comparison of *osmads1-z* and *osmads1-z osmads5-3* revealed similar phenotypes suggesting that *OsMADS1* is mostly epistatic to *OsMADS5*. However, despite the total number of second whorl organs being similar in these two mutants, the ratio of extra glume-like organs and normal lodicules was nearly halved in the double mutant, suggesting that the mutation of *OsMADS5* in the *osmads1-z* background could partially recover the defects of *osmads1-z* in the second whorl.

Compared with *osmads1-z*, *osmads1-z osmads34-1* shows slightly enhanced defects of inner floral organs, suggesting that *OsMADS34* is also involved in determining their identity redundantly with *OsMADS1* (Gao et al., 2010). In our study, more severe defects were found in the *osmads1-z osmads5-3 osmads34-1* triple mutant, compared to *osmads1-z osmads34-1*, including the enhanced elongation of leaf-like sterile lemmas and leaf-like lemma/paleas, the reduction in the number of elongated mrp-like second whorl organs, normal lodicules and reproductive organs, and defective meristem determinacy. Moreover, the total number of the leaf-like organs in the outer whorls was dramatically increased. This suggests either the homeotic transformation from the organs of the innermost three whorls to the leaf-like structures of the outer whorls, and/or the SM-to-FM transition is gravely affected in *osmads1-z osmads5-3 osmads34-1*. A previous study has shown that simultaneous knockdown of four *SEP*-like genes *OsMADS1*, *OsMADS5*, *OsMADS7(45)*, and *OsMADS8(24)* led to homeotic transformation of the lodicule and reproductive organs into leaf-like organs, while the lemma and palea were marginally affected (Cui et al., 2010). Our *osmads1-z osmads5-3 osmads34-1* triple mutant showed floral organs phenotypes very similar to those of the quadruple RNAi lines in the innermost three whorls, whereas the severe

Figure 5. (*Continued.*)
The error bars indicate the SD for three biological replications. In, inflorescence; *m1*, *osmads1-z*; *m5*, *osmads5-3*; *m34*, *osmads34-1*; ZH11, Zhonghua 11.

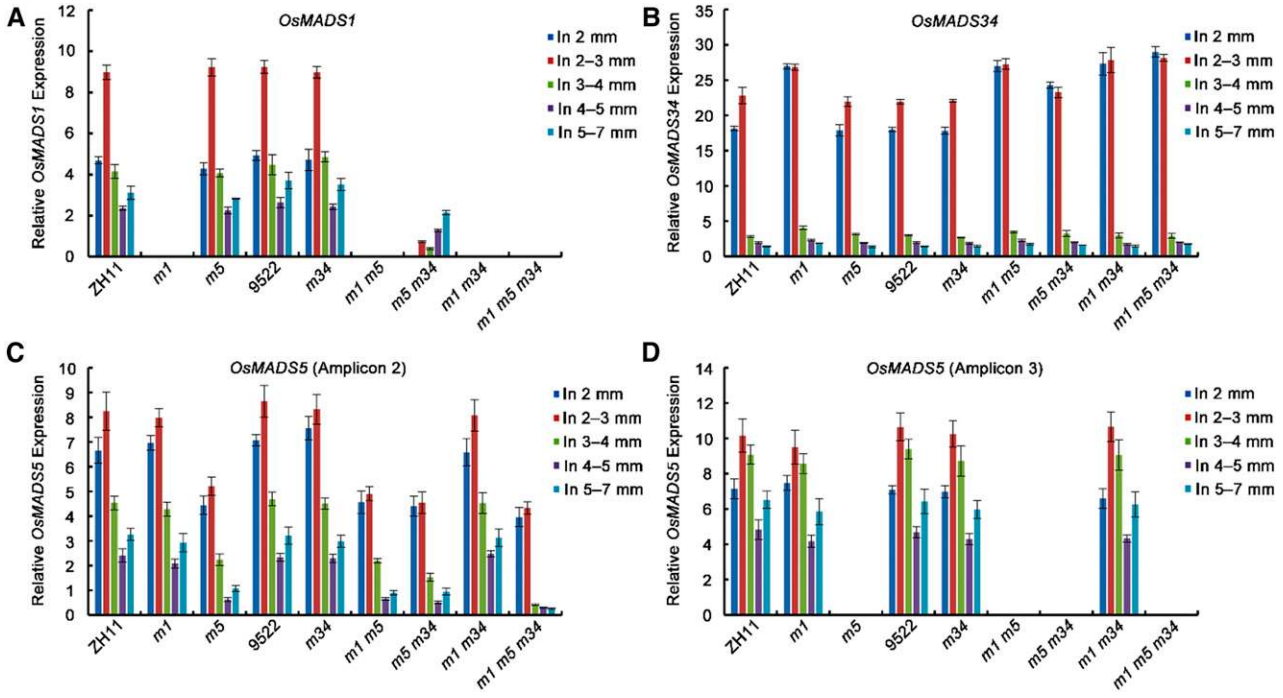

Figure 6. Expression analysis of *LOFSEP* genes in young panicles of *lofsep* mutants and wild-type backgrounds. A to D, Expression levels of *LOFSEP* genes *OsMADS1* (A), *OsMADS34* (B), and *OsMADS5* (C and D) were detected by qRT-PCR. The second and third primer pairs shown in Supplemental Figure S1A were used to quantify *OsMADS*5 transcripts upstream (C) and downstream (D) of the T-DNA insertion site, which causes the *osmads5-3* mutant, respectively. Total RNA was isolated from 2- to 7-mm young inflorescences from *lofsep* mutants and their wild-type backgrounds. The results are presented as mean ± SD. The error bars indicate the SD for three biological replications. In, inflorescence; *m1*, *osmads1-z*; *m5*, *osmads5-3*; *m34*, *osmads34-1*; ZH11, Zhonghua 11.

conversion to leaf-like organs in the outer whorls were not observed in the quadruple RNAi lines. In addition, the spikelet of *osmads1-z osmads5-3 osmads34-1* exhibited an elongated, slender, and cylindrical pattern with little empty space inside, and the average length of the elongated leaf-like sterile lemmas and leaf-like lemma/paleas were 5.03 and 4.86 times that of wild type, and 2.92 and 2.28 times that of *osmads1-z osmads34-1*, respectively (Supplemental Figs. S2 and S4, A and B), causing the *osmads1-z osmads5-3 osmads34-1* spikelets to become more like vegetative shoots. In summary, the *SEP* subfamily genes are functionally diversified in rice, with the *SEP3*-like genes showing restricted functions in the innermost three whorls, as in Arabidopsis and *Petunia x hybrida* hort. ex E.Vilm. (Mandel and Yanofsky, 1998; Pelaz et al., 2000; Ferrario et al., 2003; Vandenbussche et al., 2003; Rijpkema et al., 2009), while the function of *LOFSEP* genes starts earlier, in the specification of all spikelet and floral organs and also influencing meristem identity and determinacy as well.

Conservation and Diversification of *SEP*s in Arabidopsis and Rice

Phylogenetic analysis has revealed that the class E genes are clustered into an angiosperm-specific *SEP* subfamily that consists of two major, ubiquitous clades, called *LOFSEP* and *SEP3*, which probably arose via the whole genome duplication preceding the most recent common ancestor of angiosperms (Malcomber and Kellogg, 2005; Zahn et al., 2005). In Arabidopsis, *SEP1*, *SEP2*, and *SEP4* (*LOFSEP* clade) are expressed throughout the FM at stage 2 and continue in the primordia of all floral organs: sepals, petals, stamens, carpels, and ovules, while the expression of *SEP3* starts slightly later in late stage 2 floral primordia and continues in the inner three whorls rather than in sepals (Flanagan and Ma, 1994; Huang et al., 1995; Savidge et al., 1995; Mandel and Yanofsky, 1998; Ditta et al., 2004), suggesting that *Arabidopsis SEP* genes may encode functionally redundant proteins. In agreement with this, single *SEP* gene mutations produce only subtle or no phenotypes, while in a *sep1 sep2 sep3* triple mutant the floral organs in the innermost three whorls turn into ectopic sepals and an even more striking phenotype occurs in *sep1 sep2 sep3 sep4* quadruple mutant, where the floral organs of all four whorls are converted into leaf-like organs, indicating the central roles of the *SEP* genes in specifying FM and organ identity (Pelaz et al., 2000; Pelaz et al., 2001; Ditta et al., 2004). However, the *sep1 sep2 sep4* (*lofsep*) triple mutant shows no significant perturbation of floral organ development, suggesting that *SEP3* is significantly more critical for flower development than other *SEP*s (Ditta et al., 2004).

The expression patterns of rice *SEP3*-like genes *OsMADS7(45)* and *OsMADS8(24)* share much similarity

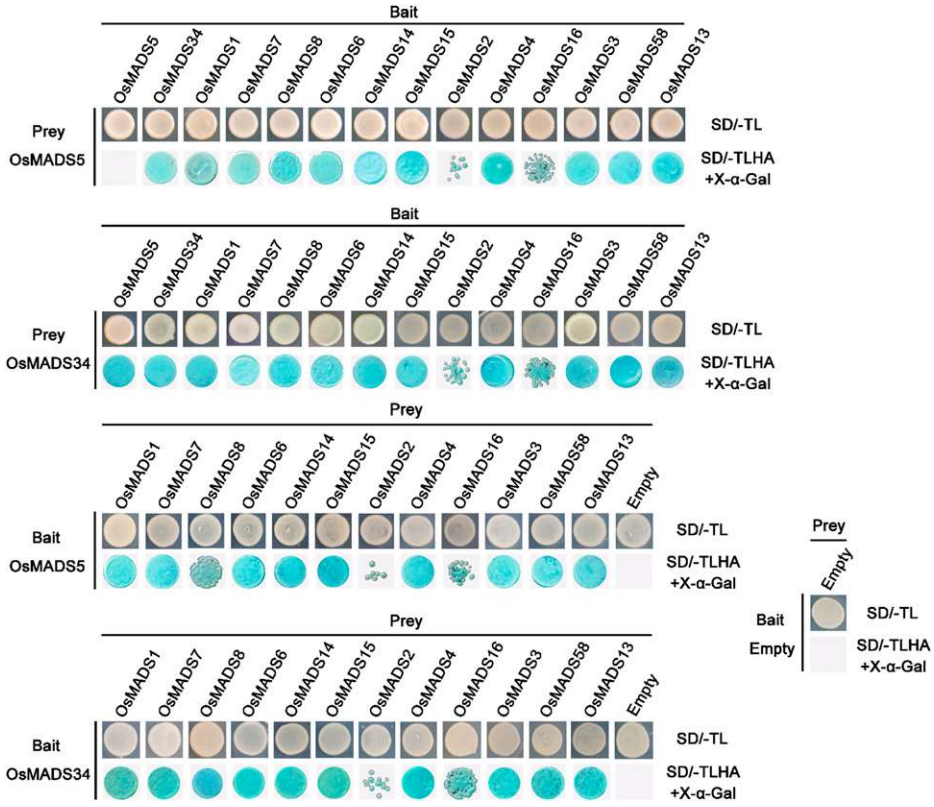

Figure 7. Interaction analysis of OsMADS5 and OsMADS34 with other floral homeotic MADS-box proteins. Yeast two-hybrid assay shows the interaction patterns of rice LOFSEP members OsMADS5 and OsMADS34 with class A (OsMADS14 and OsMADS15), class B (OsMADS2, OsMADS4 and OsMADS16), class C (OsMADS3 and OsMADS58), class D (OsMADS13), AGL6-like (OsMADS6), SEP3-like (OsMADS7 and OsMADS8), and LOFSEP-like (OsMADS1, OsMADS5, and OsMADS34) proteins, respectively. The transformants were grown on selective Minimal Synthetic Dropout (SD) media at high stringency (SD/-Ade/-His/-Leu/-Trp/X-α-Gal). Cotransformants with empty vectors pGADT7 and pGBKT7 were used as negative controls. A, adenine; H, His; L, Leu; T, Trp.

with *SEP3* in eudicots (Pelucchi et al., 2002; Cui et al., 2010), suggesting that they share similar conserved roles. Supportively, simultaneous knockdown of *OsMADS7 (45)* and *OsMADS8(24)* in rice induces strong defects specifically in whorls 2, 3, and 4 (Cui et al., 2010). Despite in situ RNA hybridization results indicating an earlier expression of *OsMADS8(24)* in the inflorescence branch meristems (Cui et al., 2010), this finding seems in contrast with independent quantitative experiments (Kobayashi et al., 2010; Harrop et al., 2016).

The expression patterns of rice *LOFSEP*-like genes are diversified compared to their orthologs *SEP1*, *SEP2*, and *SEP4* in Arabidopsis. In rice, the global expression profile of *LOFSEP* genes starts earlier than that of the *SEP3* genes and is associated with the development of the outer spikelet organs. Rice sterile lemmas, lemma, and, eventually, the palea represent new bract-like organs surrounding the flower, which evolved in the monocot grass lineage, and *LOFSEP* genes were clearly neofunctionalized and recruited to regulate their identity. This effect might be indirect and dependent on the *LOFSEP* function in SM identity specification: as the SM identity is increasingly lost in *lofsep* mutant combinations, the glumes are gradually converted toward a default leaf identity. A similar mechanism has been proposed to explain the effect of A-class mutants on sepal identity in Arabidopsis, alternatively to the existence of a true and direct A function (reviewed by Causier et al., 2010). On the other hand, rice *LOFSEP* genes continue to be expressed during the formation and growth of glume primordia. *OsMADS34* is expressed in the inflorescence meristem and branch meristems, and later in the primordia of rudimentary glumes and sterile lemmas. During later stages, *OsMADS34* is expressed in the primordia of lemma, palea, stamens, carpels, and ovules but is absent from the lodicule primordia (Gao et al., 2010; Kobayashi et al., 2010; Lin et al., 2014), although in this study we detected its expression in mature lodicules (Fig. 1C). The expression of *OsMADS5* starts in branch meristems (Kobayashi et al., 2010). In this study, we showed that *OsMADS5* is increasingly expressed in the SM and subsequently in the FM. Notably, *OsMADS5* was expressed in the primordia of all spikelet organs including the tip of rudimentary glumes and sterile lemmas, and the primordia of lemma, palea, lodicules, stamens, and carpel (Fig. 1, A and D–L). Furthermore, *OsMADS5* and *OsMADS34* showed an overlapping pattern of mRNA accumulation in all the mature spikelet organs, that is sterile lemmas, lemma, palea, lodicules, anthers, and pistil at stage In8 to In9 when the FM terminated (Fig. 1, A and C). In contrast, the transcript of *OsMADS1* is not detected during panicle branching; its earliest expression is detected in the SM, but not in the rudimentary glumes and sterile lemmas, then is confined to the lemma and palea; within the floral whorls, it is weakly expressed only in the carpel but undetectable in lodicules or stamens (Chung et al., 1994; Prasad et al., 2001; Hu et al., 2015; Fig. 1B). Despite this, the loss of *OsMADS1* function causes strong

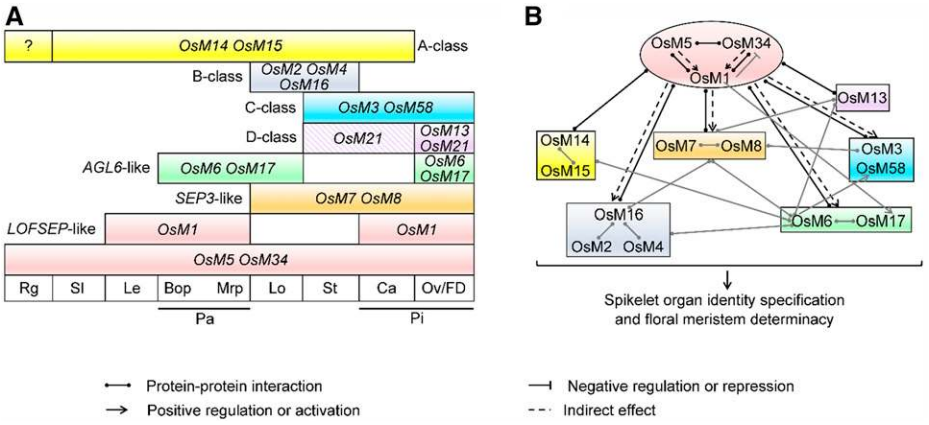

Figure 8. A working model summarizing the roles of homeotic MADS-box genes during rice spikelet development. A, The expression domains of A-, B-, C-, D-, and E-class and *AGL6*-like genes in different spikelet organs. During the spikelet development, the expression of the *FUL1*-like gene *OsMADS14* is found in the SM; later restricted to the sterile lemmas, lemma, and palea (Pelucchi et al., 2002; Preston and Kellogg, 2006, 2007); and the *FUL2*-like gene *OsMADS15* is also expressed in the SM and continues in the sterile lemmas, lemma, palea, and lodicules (Kyozuka et al., 2000; Preston and Kellogg, 2006, 2007). The *PI/GLO*-like genes *OsMADS2* and *OsMADS4* and the *AP3/DEF*-like gene *OsMADS16* share a common conserved expression domain in the lodicule and stamen primordia (Nagasawa et al., 2003; Yadav et al., 2007; Yun et al., 2013). In general, the *AG* lineage genes *OsMADS3* and *OsMADS58* exhibit a very similar expression profile in the stamen, carpel, and ovule primordia (Dreni et al., 2011). The expression of the *AGL11* lineage gene *OsMADS13* is specific in the ovule primordium (Lopez-Dee et al., 1999; Dreni et al., 2011), and yet the other *AGL11* lineage gene *OsMADS21* is expressed in the developing ovule integument and very weakly in stamens and carpels (Arora et al., 2007; Dreni et al., 2007; Dreni et al., 2011). The two *AGL6*-like genes *OsMADS6* and *OsMADS17* show a largely overlapping expression patterns in the FM and, later, in palea, lodicule, and ovule (Favaro et al., 2002; Pelucchi et al., 2002; Ohmori et al., 2009; Li et al., 2010). B, Genetic and physical interactions of MADS-box factors in regulating rice spikelet morphogenesis. Black arrows indicate the interactions presented in this study and gray arrows show the interactions reported in previous works (see manuscript text for references). Bop, body of palea; Ca, carpel; FD, floral meristem determinacy; Le, lemma; Lo, lodicule; Mrp, marginal region of palea; OsM, OsMADS; Ov, ovule; Pa, palea; Pi, pistil; Rg, rudimentary glume; Sl, sterile lemma; St, stamen.

defects in the inner floral whorls (Jeon et al., 2000; Prasad et al., 2001; Agrawal et al., 2005), demonstrating a pivotal role of *OsMADS1* in the establishment of the FM. In agreement with their expression maxima (Fig. 1, A–C), *OsMADS34* is more important for the development of sterile lemmas, whereas *OsMADS1* is required for lemma and palea development. *OsMADS5* single mutants have no phenotype; however, all three genes share significant redundancy in the development of both glumes and floral organs, as revealed by double and triple mutants. In Arabidopsis, flower development is not significantly affected even in the *lofsep* triple mutant *sep1 sep2 sep4*, whereas we have found drastic effects in the corresponding mutant of rice. In this study, the sterile lemmas, lemmas, and paleas, as well as the inner floral organs of *osmads1-z osmads5-3 osmads34-1*, were converted into leaf-like structures mimicking the phenotype of *sep1 sep2 sep3 sep4* of Arabidopsis. This demonstrates that there is a clear functional conservation of the *SEP* subfamily in the regulation of floral organ and meristem identity, but in rice we observe a higher degree of subfunctionalization.

Contrary to previous assumptions, we reveal that *OsMADS5* actively participates together with its paralogs in spikelet and floral morphogenesis. This is a significant advance in understanding the basal genetic model of flower development in rice, because, previously, *OsMADS5* was thought to play a minor role at best (Agrawal et al., 2005). Interestingly, besides its general redundancy with *OsMADS1* and *OsMADS34*, *OsMADS5* shows some antagonistic effect in the second whorl, because its mutation partially rescued the formation of extra glume-like organs in *osmads1* and *osmads1 osmads34-1* mutant backgrounds.

The main implication of the expression patterns of *SEP* genes is that, in rice, *LOFSEP* and *SEP3* genes are coexpressed with all the other MADS-box genes involved in flower development. Here, the comprehensive comparison of the expression patterns of floral homeotic MADS-box genes enabled us to construct an overarching model of expression profiles during spikelet morphogenesis (Fig. 8A). This model has facilitated the integration of previously published data with the findings of this study.

LOFSEP-Like Members of Rice Are Upstream Activators of Class B, C, D, E, and *AGL6*-Like Genes

Another key difference in rice is that the expression of *SEP3*-like genes seems to be activated by *LOFSEP*s, which is not observed in Arabidopsis. In *osmads1-z osmads5-3 osmads34-1*, the expression of *SEP3*-like genes, like one of the *AGL6*-like, B, and C genes, is

dramatically delayed and reduced during floral organogenesis from the stages of lemma primordium, FM, and palea primordium initiation (Sp3/Sp4) to the formation of floral organs and the termination of FM (Fig. 5, C–J). Yet this apparent function of *LOFSEP* genes as activators may not be absolute, as also in the triple mutant the conversion of the SM into FM is retarded not abolished, and defective or reduced floral organs still develop after several whorls of leaf-like bracts. However, because *osmads5-3* and *omads34-1* may not be knock-out mutations, this assumption needs to be verified with more alleles in the future.

In Arabidopsis, the B and C genes do not strictly depend on SEP to be activated in the floral primordium (Pelaz et al., 2000), although SEP proteins probably bind to their promoters to ensure proper expression levels (Kaufmann et al., 2009). *SEP3* itself does not appear to act downstream of *LOFSEP* genes in Arabidopsis, as in the *sep1 sep2 sep4* triple (*lofsep*) mutant is still expressed and is sufficient to provide the E function (Ditta et al., 2004). Therefore, our analysis suggests that the rice *LOFSEP* genes may regulate floral organ identity and meristem determinacy through the initial activation of all the other floral homeotic MADS-box genes. The hypothesis that these genes are direct targets of LOFSEP proteins is a likely scenario but challenging to test because of the difficulty in developing efficient antibodies for chromatin immunoprecipitation, although using this method we have previously shown that *OsMADS17*, one of the rice *AGL6*-like members, is a direct downstream target of *OsMADS1* (Hu et al., 2015). Regarding the relationship among the *LOFSEP*-like members, *OsMADS1* is down-regulated in the *osmads5-3 osmads34-1* double mutant, but the expression level of *OsMADS34* is increased in *osmads1-z*, suggesting that *OsMADS5* and *OsMADS34* may together promote *OsMADS1* during spikelet morphogenesis and that *OsMADS1* may antagonize *OsMADS34*. This is consistent with previous reports that *OsMADS1* promotes and ensures the SM to FM transition by reducing the expression of the SM identity factors such as *OsMADS34* in young spikelets, probably by direct targeting, and contributes to the maintenance of FM identity and its determinate development (Jeon et al., 2000; Agrawal et al., 2005; Prasad et al., 2005; Chen et al., 2006; Gao et al., 2010; Khanday et al., 2013; Xu et al., 2017). However, we show that the SM to FM transition is further delayed in *osmads1-z osmads5-3 osmads34-1*, suggesting that *OsMADS34* may function either as an SM or an FM identity gene, perhaps depending on the genetic context and presence of stage specific interaction partners. In addition, *OsMADS34* may repress *OsMADS1* in developing sterile lemmas, based on recent reports (Ren et al., 2016).

LOFSEP Proteins Participate in Rice Floral Quartets

The SEP proteins appear to act as the "glue" mediating the assembly of ABCD floral homeotic proteins into alternative MADS-box complexes specifying different floral whorls in eudicots (Theissen, 2001; Theissen and Saedler, 2001; Malcomber and Kellogg, 2005; Immink et al., 2009). The SEP proteins of both rice and Arabidopsis either form homodimers or heterodimers to interact with A-, B-, C-, and D-class and AGL6-like proteins (Honma and Goto, 2001; Favaro et al., 2002, 2003; Cooper et al., 2003; Lee et al., 2003; de Folter et al., 2005; Kater et al., 2006; Cui et al., 2010). For example, to date OsMADS1 has been shown to interact with OsMADS14 and OsMADS15 (A-class), OsMADS16 (B-class), OsMADS3 and OsMADS58 (C-class), OsMADS13 (D-class), OsMADS6 (AGL6-like), OsMADS7, and OsMADS8 (SEP3-like), and to form homodimers weakly (Moon et al., 1999b; Lim et al., 2000; Cui et al., 2010; Hu et al., 2015). Similarly, OsMADS34 can form homodimers, or heterodimers with OsMADS14, OsMADS15, and OsMADS18, OsMADS58, OsMADS6, and OsMADS7 (Kobayashi et al., 2012; Lin et al., 2014). In this study, we reveal that OsMADS5 and OsMADS34 have a similar ability to interact with candidate class A, B, C, D, E, and AGL6-like floral homeotic proteins. Previously, no direct interactions were detected when using the K domain of OsMADS16 or the KC domain of OsMADS4 as bait and the KC domain of OsMADS5 as prey (Moon et al., 1999a; Lee et al., 2003). Here, we observed heterodimerization using the extended IKC domain of OsMADS4 and OsMADS16, and the full-length protein of OsMADS5. These results confirmed that I and K domains are essential to mediate protein interactions while the C domain plays a crucial role in the formation of higher order complexes (Moon et al., 1999a; Causier et al., 2010; Lin et al., 2014).

Therefore, both LOFSEP and SEP3 proteins can interact with B, C, and AGL6-like proteins. Moreover, apart from the absence of *OsMADS1* in the second and third whorls, *LOFSEP* genes are consistently expressed in all floral organs, demonstrated in this work and by independent data, indicating that rice LOFSEP proteins likely participate in the formation of the putative floral quartets or of functionally equivalent complexes (Fig. 8, A and B). However, because *SEP3*-like genes are dramatically down-regulated in *lofsep* mutants, genetic tests are much more complicated in rice than in Arabidopsis and will require further studies in the future.

In summary, the MADS-box floral quartet complexes and even higher order complexes with non-MADS transcription factors may also be formed in rice and other monocots, similar to those surmised in core eudicots (West et al., 1998; Egea-Cortines et al., 1999; West and Sharrocks, 1999; Honma and Goto, 2001; Theissen and Saedler, 2001). In yeast two-hybrid screenings using LOFSEP proteins as baits, the AP1/FUL-like proteins OsMADS14 and OsMADS15 emerged as the MADS-box factors with the highest affinity (Lim et al., 2000; Q. Meng, W. Liang, and D. Zhang, unpublished data). Their encoding genes are coexpressed with *LOFSEP* genes in both SMs and FMs. Interestingly, a recent analysis of these two

transcription factors underlined their essential role in inflorescence development and spikelet development (Wu et al., 2017), with double mutants showing leafy-like bracts, papery lodicules, and other floral defects reminiscent of the *osmads1-z osmads5-3 osmads34-1* phenotype. The combination of previous data and molecular models predicting SEP-AP1 complexes as activators of B and C function genes in Arabidopsis (Honma and Goto, 2001; de Folter et al., 2005; Gregis et al., 2009), and the higher order mutants between *AP1*, *CAL*, *SEP1/2/4* as well as *SEP4* overexpression, confirmed that the *LOFSEP* genes of Arabidopsis are indeed promoters of FM identity (Ditta et al., 2004). The results presented here suggest that the same mechanism has been only partially rewired during the evolution of grass reproductive organs.

MATERIALS AND METHODS

Plant Materials

The three rice single mutants *osmads5-3*, *osmads1-z*, and *osmads34-1* were used in this study. Subsequently, three CRISPR/Cas9 lines *osmads5(M)-CRISPR*, *osmads5(I)-CRISPR*, and *osmads34(I)-CRISPR* were developed to confirm the mutant phenotypes. The parental cultivar of *osmads5-3* and *osmads1-z* is Zhonghua11 (*Oryza sativa* L. ssp. *japonica*) while for *osmads34-1*, *osmads5(M)-CRISPR*, *osmads5(I)-CRISPR*, and *osmads34(I)-CRISPR* it is 9522 (*Oryza sativa* L. ssp. *japonica*). Both *osmads1-z* and *osmads34-1* have been previously described by our group (Gao et al., 2010; Hu et al., 2015). Double and triple mutants were isolated by genotyping and phenotype observation. All plant materials used in this study were grown in the paddy field at Shanghai Jiao Tong University (at 31°2′3.55′′ North latitude, 121°26′39.70′′ East longitude) from May to September.

Genotyping of *lofsep* Mutant Plants

For genotyping the T-DNA line *osmads5-3*, the PCR primer set OsM5 GF and OsM5 GR was used to detect the *OsMADS5* wild-type allele and OsM5 GF with NTLB5 for the *osmads5-3* allele. For the CRISPR mutant lines *osmads5(M)-CRISPR*, *osmads5(I)-CRISPR* and *osmads34(I)-CRISPR*, the genotyping was performed by PCR amplification and sequencing using three primer sets OsM5-C G1F and OsM5-C G1R, OsM5-C G2F and OsM5-C G2R, and OsM34-C GF and OsM34-C GR, respectively. The genotyping of *osmads1-z* and *osmads34-1* plants was described previously (Gao et al., 2010; Hu et al., 2015). All primers are listed in Supplemental Table S8.

Morphological Analysis and Microscopy Observation

Fresh spikelets at stage In9 were photographed with a Leica stereomicroscope (S8AP0). For cytological analysis, young spikelets of mutants and wild type were fixed in fresh FAA solution (50% ethanol, 5% acetic acid, and 3.7% formaldehyde) and dehydrated through a series of graded ethanol solutions (70% twice, 80%, 90% and 95% once each, and 100% twice). Samples for paraffin sectioning were infiltrated with Histo-Clear II, embedded in Paraplast Plus, sectioned into 6-μm-thick slices using a Leica rotary microtomes (RM2245), deparaffinized, and photographed under a Nikon microscope (Eclipse 80i). The samples for SEM were prepared and analyzed as described previously (Li et al., 2006).

cDNA Preparation and qRT-PCR Analysis

For the expression analysis of *OsMADS1*, *OsMADS5*, and *OsMADS34*, total RNA of three biological replicates was extracted using Trizol Reagent (Invitrogen) from young panicles between 0.3 to 7 mm long, thus covering broad inflorescence and spikelet developmental stages of In4, In5 and Sp1 to Sp8, and also from mature sterile lemmas, lemmas, paleas, lodicules, anthers, and pistils at stage In8 to In9.

To analyze the expression of floral homeotic genes in *lofsep* mutants, young inflorescences from 2 mm to 7 mm long were harvested from the *lofsep* mutants and from the wild type, covering five time-points across spikelet development. Indeed a 2-mm-long inflorescence in the wild-type cultivars Zhonghua11 or 9522 has mostly spikelet primordia at the Sp4 stage, with a few still at stage Sp3. When the inflorescence length becomes 2 to 3 mm, most of the spikelet primordia are at Sp5, with a small number at Sp4 or Sp6. Similarly, we sampled inflorescences at 3 to 4 mm, 4 to 5 mm, or 5 to 7 mm long, which mostly bear stage Sp6, Sp7, and Sp8 spikelet primordia, respectively.

The cDNA was synthesized using the PrimeScript RT reagent Kit with gDNA Eraser (Takara). The qRT-PCR analysis was performed using the CFX96 Real-Time PCR Detection System (Bio-Rad) with SuperReal PreMix Plus (SYBR Green, TIANGEN). Primers for *OsMADS16*, *OsMADS58*, *OsMADS7*, and *OsMADS8* were described by (Cui et al., 2010); *OsMADS4*, *OsMADS17*, and *OsMADS1* by (Hu et al., 2015); *OsMADS3* by (Chen et al., 2006); *OsMADS6* by (Ohmori et al., 2009); and *OsMADS34* by (Gao et al., 2010). All primers are listed in Supplemental Table S8. Data were processed using the CFX Manager software and Excel, based on the relative quantitation delta-delta Ct method.

RNA In Situ Hybridization

Fresh young panicles dissected from wild type were fixed immediately in FAA solution, then dehydrated, infiltrated, embedded, and sectioned as described above in the paraffin section method. The digoxygenin-labeled gene-specific RNA probes of *OsMADS5* were generated in vitro from a cDNA PCR amplicon comprising the C terminal of coding region and the 3′-UTR region of *OsMADS5*. Primers for in situ hybridization are listed in Supplemental Table S8. Digoxygenin-labeled RNA hybridization and hybridized probes detection were performed essentially according to (Dreni et al., 2007). Images were captured on a Nikon microscope (Eclipse 80i).

Yeast Two-Hybrid Assay

The full-length cDNAs of *OsMADS5*, *OsMADS34*, *OsMADS1*, *OsMADS7*, *OsMADS8*, *OsMADS14*, *OsMADS15*, and *OsMADS58*; the cDNA fragments encoding the IKC domains of *OsMADS2*, *OsMADS4*, *OsMADS16*, *OsMADS3*, *OsMADS13*; and the cDNA fragments encoding the MIK domains as well as the first 14 amino acid residues of C domains of *OsMADS6* were amplified and cloned into both the activation-domain vector pGADT7 and the DNA-binding domain vector pGBKT7 (Clontech). Yeast two-hybrid assay was subsequently performed according to the MATCHMAKER GAL4 Two-Hybrid System 3 & Libraries User Manual (Clontech). Protein interactions were tested and no single constructs gave rise to detectable autonomous activation as indicated by yeast growth ability on selective Minimal Synthetic Dropout media with high stringency (Minimal Synthetic Dropout/-Ade/-His/-Leu/-Trp/X-α-Gal). The transformants containing empty plasmids of both pGADT7 and pGBKT7 were used as negative controls.

Accession Numbers

Sequence data from this article can be found in the Rice Genome Annotation Project Database under the following accession numbers: *OsMADS5* (Os06g06750), *OsMADS1* (Os03g11614), *OsMADS34* (Os03g54170), *OsMADS7* (Os08g41950), *OsMADS8* (Os09g32948), *OsMADS6* (Os02g45770), *OsMADS17* (Os04g49150), *OsMADS14* (Os03g54160), *OsMADS15* (Os07g01820), *OsMADS2* (Os01g66030), *OsMADS4* (Os05g34940), *OsMADS16* (Os06g49840), *OsMADS3* (Os01g10504), *OsMADS58* (Os05g11414), and *OsMADS13* (Os12g10540).

Supplemental Data

The following supplemental materials are available.

Supplemental Figure S1. The *osmads5* and *osmads34* mutant alleles.

Supplemental Figure S2. Spikelets of *lofsep* mutants and of the wild-type parental cultivars.

Supplemental Figure S3. SEM analysis of spikelet primordia from wild type and *lofsep* mutants.

Supplemental Figure S4. Statistics of spikelet organs of *lofsep* mutants and the wild type.

Supplemental Figure S5. Phenotypes of wild-type, *osmads5*, and *osmads34* CRISPR lines.

Supplemental Table S1. The number and percentage of floral organs of the *osmads5-3*, *osmads34-1*, and *osmads5-3 osmads34-1* mutants.

Supplemental Table S2. The classification and percentage of five types of phenotypes presented by *osmads1-z* and *osmads1-z osmads5-3* mutants.

Supplemental Table S3. The number and percentage of spikelet organs of *osmads1-z* and *osmads1-z osmads5-3* mutants.

Supplemental Table S4. The number of spikelet organs of *osmads1-z osmads34-1* and *osmads1-z osmads5-3 osmads34-1* mutants.

Supplemental Table S5. The number of vascular bundles of *lofsep* mutants.

Supplemental Table S6. The floral organ number of the CRISPR mutants of *OsMADS5* and *OsMADS34* compared to *osmads5-3* and *osmads34-1*.

Supplemental Table S7. The number of vascular bundles of the CRISPR mutants of *OsMADS5* and *OsMADS34* compared to *osmads5-3* and *osmads34-1*.

Supplemental Table S8. Primers used in this study.

ACKNOWLEDGMENTS

We thank the staff of Rice Mutant Database for providing *osmads5-3*, Professor Hongwei Xue for providing *osmads1-z*, Zhijing Luo for rice cultivation and crosses, Changsong Yin and Jie Wang for technical assistance during in situ hybridization experiments, and Xiaonan Nie for the genotyping of *osmads5-3*.

Received May 25, 2017; accepted December 4, 2017; published December 7, 2017.

LITERATURE CITED

Agrawal GK, Abe K, Yamazaki M, Miyao A, Hirochika H (2005) Conservation of the E-function for floral organ identity in rice revealed by the analysis of tissue culture-induced loss-of-function mutants of the OsMADS1 gene. Plant Mol Biol **59:** 125–135

Arora R, Agarwal P, Ray S, Singh AK, Singh VP, Tyagi AK, Kapoor S (2007) MADS-box gene family in rice: genome-wide identification, organization and expression profiling during reproductive development and stress. BMC Genomics **8:** 242

Causier B, Schwarz-Sommer Z, Davies B (2010) Floral organ identity: 20 years of ABCs. Semin Cell Dev Biol **21:** 73–79

Chen ZX, Wu JG, Ding WN, Chen HM, Wu P, Shi CH (2006) Morphogenesis and molecular basis on naked seed rice, a novel homeotic mutation of OsMADS1 regulating transcript level of AP3 homologue in rice. Planta **223:** 882–890

Chung YY, Kim SR, Finkel D, Yanofsky MF, An G (1994) Early flowering and reduced apical dominance result from ectopic expression of a rice MADS box gene. Plant Mol Biol **26:** 657–665

Ciaffi M, Paolacci AR, Tanzarella OA, Porceddu E (2011) Molecular aspects of flower development in grasses. Sex Plant Reprod **24:** 247–282

Coen ES, Meyerowitz EM (1991) The war of the whorls: genetic interactions controlling flower development. Nature **353:** 31–37

Cooper B, Clarke JD, Budworth P, Kreps J, Hutchison D, Park S, Guimil S, Dunn M, Luginbühl P, Ellero C, et al (2003) A network of rice genes associated with stress response and seed development. Proc Natl Acad Sci USA **100:** 4945–4950

Cui R, Han J, Zhao S, Su K, Wu F, Du X, Xu Q, Chong K, Theissen G, Meng Z (2010) Functional conservation and diversification of class E floral homeotic genes in rice (Oryza sativa). Plant J **61:** 767–781

de Folter S, Immink RG, Kieffer M, Parenicová L, Henz SR, Weigel D, Busscher M, Kooiker M, Colombo L, Kater MM, et al(2005) Comprehensive interaction map of the Arabidopsis MADS Box transcription factors. Plant Cell **17:** 1424–1433

Ditta G, Pinyopich A, Robles P, Pelaz S, Yanofsky MF (2004) The SEP4 gene of Arabidopsis thaliana functions in floral organ and meristem identity. Curr Biol **14:** 1935–1940

Dreni L, Jacchia S, Fornara F, Fornari M, Ouwerkerk PB, An G, Colombo L, Kater MM (2007) The D-lineage MADS-box gene OsMADS13 controls ovule identity in rice. Plant J **52:** 690–699

Dreni L, Pilatone A, Yun D, Erreni S, Pajoro A, Caporali E, Zhang D, Kater MM (2011) Functional analysis of all AGAMOUS subfamily members in rice reveals their roles in reproductive organ identity determination and meristem determinacy. Plant Cell **23:** 2850–2863

Dreni L, Zhang D (2016) Flower development: the evolutionary history and functions of the AGL6 subfamily MADS-box genes. J Exp Bot **67:** 1625–1638

Egea-Cortines M, Saedler H, Sommer H (1999) Ternary complex formation between the MADS-box proteins SQUAMOSA, DEFICIENS and GLOBOSA is involved in the control of floral architecture in Antirrhinum majus. EMBO J **18:** 5370–5379

Favaro R, Immink RG, Ferioli V, Bernasconi B, Byzova M, Angenent GC, Kater M, Colombo L (2002) Ovule-specific MADS-box proteins have conserved protein-protein interactions in monocot and dicot plants. Mol Genet Genomics **268:** 152–159

Favaro R, Pinyopich A, Battaglia R, Kooiker M, Borghi L, Ditta G, Yanofsky MF, Kater MM, Colombo L (2003) MADS-box protein complexes control carpel and ovule development in Arabidopsis. Plant Cell **15:** 2603–2611

Ferrario S, Immink RG, Shchennikova A, Busscher-Lange J, Angenent GC (2003) The MADS box gene FBP2 is required for SEPALLATA function in petunia. Plant Cell **15:** 914–925

Flanagan CA, Ma H (1994) Spatially and temporally regulated expression of the MADS-box gene AGL2 in wild-type and mutant Arabidopsis flowers. Plant Mol Biol **26:** 581–595

Fornara F, Parenicová L, Falasca G, Pelucchi N, Masiero S, Ciannamea S, Lopez-Dee Z, Altamura MM, Colombo L, Kater MM (2004) Functional characterization of OsMADS18, a member of the AP1/SQUA subfamily of MADS box genes. Plant Physiol **135:** 2207–2219

Gao X, Liang W, Yin C, Ji S, Wang H, Su X, Guo C, Kong H, Xue H, Zhang D (2010) The SEPALLATA-like gene OsMADS34 is required for rice inflorescence and spikelet development. Plant Physiol **153:** 728–740

Greco R, Stagi L, Colombo L, Angenent GC, Sari-Gorla M, Pè ME (1997) MADS box genes expressed in developing inflorescences of rice and sorghum. Mol Gen Genet **253:** 615–623

Gregis V, Sessa A, Dorca-Fornell C, Kater MM (2009) The Arabidopsis floral meristem identity genes AP1, AGL24 and SVP directly repress class B and C floral homeotic genes. Plant J **60:** 626–637

Harrop TW, Ud Din I, Gregis V, Osnato M, Jouannic S, Adam H, Kater MM (2016) Gene expression profiling of reproductive meristem types in early rice inflorescences by laser microdissection. Plant J **86:** 75–88

Honma T, Goto K (2001) Complexes of MADS-box proteins are sufficient to convert leaves into floral organs. Nature **409:** 525–529

Hu L, Liang W, Yin C, Cui X, Zong J, Wang X, Hu J, Zhang D (2011) Rice MADS3 regulates ROS homeostasis during late anther development. Plant Cell **23:** 515–533

Hu Y, Liang W, Yin C, Yang X, Ping B, Li A, Jia R, Chen M, Luo Z, Cai Q, et al (2015) Interactions of OsMADS1 with floral homeotic genes in rice flower development. Mol Plant **8:** 1366–1384

Huang H, Tudor M, Weiss CA, Hu Y, Ma H (1995) The Arabidopsis MADS-box gene AGL3 is widely expressed and encodes a sequence-specific DNA-binding protein. Plant Mol Biol **28:** 549–567

Ikeda K, Sunohara H, Nagato Y (2004) Developmental course of inflorescence and spikelet in rice. Breed Sci **54:** 147–156

Immink RG, Tonaco IA, de Folter S, Shchennikova A, van Dijk AD, Busscher-Lange J, Borst JW, Angenent GC (2009) SEPALLATA3: the 'glue' for MADS box transcription factor complex formation. Genome Biol **10:** R24

Itoh J, Nonomura K, Ikeda K, Yamaki S, Inukai Y, Yamagishi H, Kitano H, Nagato Y (2005) Rice plant development: from zygote to spikelet. Plant Cell Physiol **46:** 23–47

Jeon JS, Jang S, Lee S, Nam J, Kim C, Lee SH, Chung YY, Kim SR, Lee YH, Cho YG, et al (2000) leafy hull sterile1 is a homeotic mutation in a rice MADS box gene affecting rice flower development. Plant Cell **12:** 871–884

Kang HG, Jang S, Chung JE, Cho YG, An G (1997) Characterization of two rice MADS box genes that control flowering time. Mol Cells **7:** 559–566

Kang HG, Jeon JS, Lee S, An G (1998) Identification of class B and class C floral organ identity genes from rice plants. Plant Mol Biol **38:** 1021–1029

Kater MM, Dreni L, Colombo L (2006) Functional conservation of MADS-box factors controlling floral organ identity in rice and Arabidopsis. J Exp Bot **57:** 3433–3444

Kaufmann K, Muiño JM, Jauregui R, Airoldi CA, Smaczniak C, Krajewski P, Angenent GC (2009) Target genes of the MADS

transcription factor SEPALLATA3: integration of developmental and hormonal pathways in the Arabidopsis flower. PLoS Biol **7:** e1000090

Kellogg EA (2001) Evolutionary history of the grasses. Plant Physiol **125:** 1198–1205

Khanday I, Yadav SR, Vijayraghavan U (2013) Rice LHS1/OsMADS1 controls floret meristem specification by coordinated regulation of transcription factors and hormone signaling pathways. Plant Physiol **161:** 1970–1983

Kobayashi K, Maekawa M, Miyao A, Hirochika H, Kyozuka J (2010) PANICLE PHYTOMER2 (PAP2), encoding a SEPALLATA subfamily MADS-box protein, positively controls spikelet meristem identity in rice. Plant Cell Physiol **51:** 47–57

Kobayashi K, Yasuno N, Sato Y, Yoda M, Yamazaki R, Kimizu M, Yoshida H, Nagamura Y, Kyozuka J (2012) Inflorescence meristem identity in rice is specified by overlapping functions of three AP1/FUL-like MADS box genes and PAP2, a SEPALLATA MADS box gene. Plant Cell **24:** 1848–1859

Kyozuka J, Kobayashi T, Morita M, Shimamoto K (2000) Spatially and temporally regulated expression of rice MADS box genes with similarity to Arabidopsis class A, B and C genes. Plant Cell Physiol **41:** 710–718

Kyozuka J, Shimamoto K (2002) Ectopic expression of OsMADS3, a rice ortholog of AGAMOUS, caused a homeotic transformation of lodicules to stamens in transgenic rice plants. Plant Cell Physiol **43:** 130–135

Lee S, Jeon JS, An K, Moon YH, Lee S, Chung YY, An G (2003) Alteration of floral organ identity in rice through ectopic expression of OsMADS16. Planta **217:** 904–911

Li H, Liang W, Hu Y, Zhu L, Yin C, Xu J, Dreni L, Kater MM, Zhang D (2011) Rice MADS6 interacts with the floral homeotic genes SUPERWOMAN1, MADS3, MADS58, MADS13, and DROOPING LEAF in specifying floral organ identities and meristem fate. Plant Cell **23:** 2536–2552

Li H, Liang W, Jia R, Yin C, Zong J, Kong H, Zhang D (2010) The AGL6-like gene OsMADS6 regulates floral organ and meristem identities in rice. Cell Res **20:** 299–313

Li N, Zhang DS, Liu HS, Yin CS, Li XX, Liang WQ, Yuan Z, Xu B, Chu HW, Wang J, et al (2006) The rice tapetum degeneration retardation gene is required for tapetum degradation and anther development. Plant Cell **18:** 2999–3014

Lim J, Moon YH, An G, Jang SK (2000) Two rice MADS domain proteins interact with OsMADS1. Plant Mol Biol **44:** 513–527

Lin X, Wu F, Du X, Shi X, Liu Y, Liu S, Hu Y, Theißen G, Meng Z (2014) The pleiotropic SEPALLATA-like gene OsMADS34 reveals that the 'empty glumes' of rice (Oryza sativa) spikelets are in fact rudimentary lemmas. New Phytol **202:** 689–702

Linder HP, Rudall PJ (2005) Evolutionary history of poales. Annu Rev Ecol Evol Syst **36:** 107–124

Lopez-Dee ZP, Wittich P, Enrico Pè M, Rigola D, Del Buono I, Gorla MS, Kater MM, Colombo L (1999) OsMADS13, a novel rice MADS-box gene expressed during ovule development. Dev Genet **25:** 237–244

Malcomber ST, Kellogg EA (2005) SEPALLATA gene diversification: brave new whorls. Trends Plant Sci **10:** 427–435

Mandel MA, Yanofsky MF (1998) The ArabidopsisAGL9 MADS box gene is expressed in young flower primordia. Sex Plant Reprod **11:** 22–28

Moon YH, Jung JY, Kang HG, An G (1999a) Identification of a rice APETALA3 homologue by yeast two-hybrid screening. Plant Mol Biol **40:** 167–177

Moon YH, Kang HG, Jung JY, Jeon JS, Sung SK, An G (1999b) Determination of the motif responsible for interaction between the rice APETALA1/AGAMOUS-LIKE9 family proteins using a yeast two-hybrid system. Plant Physiol **120:** 1193–1204

Nagasawa N, Miyoshi M, Sano Y, Satoh H, Hirano H, Sakai H, Nagato Y (2003) SUPERWOMAN1 and DROOPING LEAF genes control floral organ identity in rice. Development **130:** 705–718

Ohmori S, Kimizu M, Sugita M, Miyao A, Hirochika H, Uchida E, Nagato Y, Yoshida H (2009) MOSAIC FLORAL ORGANS1, an AGL6-like MADS box gene, regulates floral organ identity and meristem fate in rice. Plant Cell **21:** 3008–3025

Pelaz S, Ditta GS, Baumann E, Wisman E, Yanofsky MF (2000) B and C floral organ identity functions require SEPALLATA MADS-box genes. Nature **405:** 200–203

Pelaz S, Tapia-López R, Alvarez-Buylla ER, Yanofsky MF (2001) Conversion of leaves into petals in Arabidopsis. Curr Biol **11:** 182–184

Pelucchi N, Fornara F, Favalli C, Masiero S, Lago C, Pè EM, Colombo L, Kater MM (2002) Comparative analysis of rice MADS-box genes expressed during flower development. Sex Plant Reprod **15:** 113–122

Pinyopich A, Ditta GS, Savidge B, Liljegren SJ, Baumann E, Wisman E, Yanofsky MF (2003) Assessing the redundancy of MADS-box genes during carpel and ovule development. Nature **424:** 85–88

Prasad K, Parameswaran S, Vijayraghavan U (2005) OsMADS1, a rice MADS-box factor, controls differentiation of specific cell types in the lemma and palea and is an early-acting regulator of inner floral organs. Plant J **43:** 915–928

Prasad K, Sriram P, Kumar CS, Kushalappa K, Vijayraghavan U (2001) Ectopic expression of rice OsMADS1 reveals a role in specifying the lemma and palea, grass floral organs analogous to sepals. Dev Genes Evol **211:** 281–290

Prasad K, Vijayraghavan U (2003) Double-stranded RNA interference of a rice PI/GLO paralog, OsMADS2, uncovers its second-whorl-specific function in floral organ patterning. Genetics **165:** 2301–2305

Preston JC, Kellogg EA (2006) Reconstructing the evolutionary history of paralogous APETALA1/FRUITFULL-like genes in grasses (Poaceae). Genetics **174:** 421–437

Preston JC, Kellogg EA (2007) Conservation and divergence of APETALA1/FRUITFULL-like gene function in grasses: evidence from gene expression analyses. Plant J **52:** 69–81

Ren D, Rao Y, Leng Y, Li Z, Xu Q, Wu L, Qiu Z, Xue D, Zeng D, Hu J, et al (2016) Regulatory role of OsMADS34 in the determination of glumes fate, grain yield, and quality in rice. Front Plant Sci **7:** 1853

Rijpkema AS, Zethof J, Gerats T, Vandenbussche M (2009) The petunia AGL6 gene has a SEPALLATA-like function in floral patterning. Plant J **60:** 1–9

Savidge B, Rounsley SD, Yanofsky MF (1995) Temporal relationship between the transcription of two Arabidopsis MADS box genes and the floral organ identity genes. Plant Cell **7:** 721–733

The Plant List (2013) Version 1.1. http://www.theplantlist.org/ (January 2, 2017)

Theissen G (2001) Development of floral organ identity: stories from the MADS house. Curr Opin Plant Biol **4:** 75–85

Theissen G, Melzer R (2007) Molecular mechanisms underlying origin and diversification of the angiosperm flower. Ann Bot **100:** 603–619

Theissen G, Saedler H (2001) Plant biology. Floral quartets. Nature **409:** 469–471

Thompson BE, Bartling L, Whipple C, Hall DH, Sakai H, Schmidt R, Hake S (2009) bearded-ear encodes a MADS box transcription factor critical for maize floral development. Plant Cell **21:** 2578–2590

Vandenbussche M, Zethof J, Souer E, Koes R, Tornielli GB, Pezzotti M, Ferrario S, Angenent GC, Gerats T (2003) Toward the analysis of the petunia MADS box gene family by reverse and forward transposon insertion mutagenesis approaches: B, C, and D floral organ identity functions require SEPALLATA-like MADS box genes in petunia. Plant Cell **15:** 2680–2693

West AG, Causier BE, Davies B, Sharrocks AD (1998) DNA binding and dimerisation determinants of Antirrhinum majus MADS-box transcription factors. Nucleic Acids Res **26:** 5277–5287

West AG, Sharrocks AD (1999) MADS-box transcription factors adopt alternative mechanisms for bending DNA. J Mol Biol **286:** 1311–1323

Wu F, Shi X, Lin X, Liu Y, Chong K, Theißen G, Meng Z (2017) The ABCs of flower development: mutational analysis of AP1/FUL-like genes in rice provides evidence for a homeotic (A)-function in grasses. Plant J **89:** 310–324

Xu W, Tao J, Chen M, Dreni L, Luo Z, Hu Y, Liang W, Zhang D (2017) Interactions between FLORAL ORGAN NUMBER4 and floral homeotic genes in regulating rice flower development. J Exp Bot **68:** 483–498

Yadav SR, Prasad K, Vijayraghavan U (2007) Divergent regulatory OsMADS2 functions control size, shape and differentiation of the highly derived rice floret second-whorl organ. Genetics **176:** 283–294

Yamaguchi T, Lee DY, Miyao A, Hirochika H, An G, Hirano HY (2006) Functional diversification of the two C-class MADS box genes OSMADS3 and OSMADS58 in Oryza sativa. Plant Cell **18:** 15–28

Yao SG, Ohmori S, Kimizu M, Yoshida H (2008) Unequal genetic redundancy of rice PISTILLATA orthologs, OsMADS2 and OsMADS4, in lodicule and stamen development. Plant Cell Physiol **49:** 853–857

Yoshida H, Itoh J, Ohmori S, Miyoshi K, Horigome A, Uchida E, Kimizu M, Matsumura Y, Kusaba M, Satoh H, et al (2007) superwoman1-

cleistogamy, a hopeful allele for gene containment in GM rice. Plant Biotechnol J **5:** 835–846

Yoshida H, Nagato Y (2011) Flower development in rice. J Exp Bot **62:** 4719–4730

Yun D, Liang W, Dreni L, Yin C, Zhou Z, Kater MM, Zhang D (2013) OsMADS16 genetically interacts with OsMADS3 and OsMADS58 in specifying floral patterning in rice. Mol Plant **6:** 743–756

Zahn LM, Kong H, Leebens-Mack JH, Kim S, Soltis PS, Landherr LL, Soltis DE, Depamphilis CW, Ma H (2005) The evolution of the SEPALLATA subfamily of MADS-box genes: a preangiosperm origin with multiple duplications throughout angiosperm history. Genetics **169:** 2209–2223

Zhang D, Wilson ZA (2009) Stamen specification and anther development in rice. Chin Sci Bull **54:** 2342–2353

Zhang D, Yuan Z (2014) Molecular control of grass inflorescence development. Annu Rev Plant Biol **65:** 553–578

Zhang D, Yuan Z, An G, Dreni L, Hu J, Kater MM (2013) Panicle development. *In* Q Zhang, RA Wing, eds, Genetics and Genomics of Rice. Springer, New York, NY, pp 279–295

Zhang J, Nallamilli BR, Mujahid H, Peng Z (2010) OsMADS6 plays an essential role in endosperm nutrient accumulation and is subject to epigenetic regulation in rice (Oryza sativa). Plant J **64:** 604–617